

# Elementary Excitations of Ferromagnetic Metal Nanoparticles

A. Cehovin

*Division of Solid State Theory, Department of Physics, Lund University, SE-223 62 Lund, Sweden*

C.M. Canali

*Department of Technology, Kalmar University, 391 82 Kalmar*

A.H. MacDonald

*Department of Physics, University of Texas at Austin, Austin TX 78712*

(Dated: July 23, 2018)

We present a theory of the elementary spin excitations in transition metal ferromagnet nanoparticles which achieves a unified and consistent quantum description of both collective and quasiparticle physics. The theory starts by recognizing the essential role played by spin-orbit interactions in determining the energies of ferromagnetic resonances in the collective excitation spectrum and the strength of their coupling to low-energy particle-hole excitations. We argue that a crossover between Landau-damped ferromagnetic resonance and pure-state collective magnetic excitations occurs as the number of atoms in typical transition metal ferromagnet nanoparticles drops below approximately  $10^4$ , approximately where the single-particle level spacing,  $\delta$ , becomes larger than  $\sqrt{\alpha}E_{\text{res}}$ , where  $E_{\text{res}}$  is the ferromagnetic resonance frequency and  $\alpha$  is the Gilbert damping parameter. We illustrate our ideas by studying the properties of semi-realistic model Hamiltonians, which we solve numerically for nanoparticles containing several hundred atoms. For small nanoparticles, we find one isolated ferromagnetic resonance collective mode below the lowest particle-hole excitation energy, at  $E_{\text{res}} \approx 0.1$  meV. The spectral weight of this pure excitation nearly exhausts the transverse dynamical susceptibility spectral weight. As  $\delta$  approaches  $\sqrt{\alpha}E_{\text{res}}$ , the ferromagnetic collective excitation is more likely to couple strongly with discrete particle-hole excitations. In this regime the distinction between the two types of excitations blurs. We discuss the significance of this picture for the interpretation of recent single-electron tunneling experiments.

## I. INTRODUCTION

In bulk condensed matter systems, normal metals are Fermi liquids; their low-energy excitation spectra can be placed in one-to-one correspondence with those of corresponding non-interacting electron systems as argued by Landau more than 50 years ago. Recent single-electron tunneling spectroscopy studies of metallic nanoparticles [1], in which the discrete excitation spectra of small systems containing less than one thousand to tens of thousands of atoms are investigated, have allowed Landau's enormous simplification of interacting fermion physics to be examined quite directly. With a few caveats and some exceptions, the wide variety of interesting phenomena that have been studied using single-electron tunneling spectroscopy can be understood using ideas from independent particle quantum mechanics. Although they can still be regarded as Fermi liquids for many purposes, metals with nearly continuous broken symmetries (in particular the ferromagnetic transition metals that are the focus of this article) support low-energy collective excitations in addition to Landau's particle-hole excitations. When spin-orbit coupling is neglected, the broken symmetry of itinerant electron ferromagnets is continuous and the collective excitations are Goldstone bosons whose energy vanishes in the long-wavelength limit. Recent single-electron tunneling spectroscopy studies [2, 3] have for the first time succeeded in resolving the excitation spectra of ferromagnetic transition metal nanoparticles with di-

ameters below 4 nm. The discrete resonances seen in the tunneling experiments measure the low-energy many-electron excitation spectra of a single-domain ferromagnetic nanoparticle. The ultimate objective of this paper is to shed light on the physics that is responsible for the rich and complex behavior seen experimentally, which includes hysteretic behavior, non-monotonic field dependences, and a much denser low-energy excitation spectrum than would be expected based on a non-interacting quasiparticle model. Our approach is based on a weak-coupling description of a metallic ferromagnet in which spin-orbit interactions cause collective and particle-hole excitation to be coupled at low-energies, and the classical micromagnetic description of a ferromagnetic metal nanoparticle emerges naturally when quantum effects are unimportant.

Our theory builds on earlier work [4, 5], which captures several features of the experimental spectra, especially when non-equilibrium excitations [6] are considered, but does not provide a unified and consistent quantum description of how collective and quasi-particle excitations are coupled by spin-orbit interactions. The purpose of this paper is to develop such a description and illustrate its implications by applying a simplified but qualitatively realistic microscopic model that we have recently introduced [7].

The elementary spin excitations in bulk itinerant-electron ferromagnets are of two kinds: collective spin excitations (spin-waves) and spin-flip particle-hole exci-

tations (Stoner excitations). Spin-wave excitations are related to the collective magnetization degree of freedom and form a branch in  $q - \omega$  space, which is gapless if the system is isotropic in accord with Goldstone's theorem. The main effects of spin-orbit interactions in the bulk are to generate an energy gap  $E_{\text{res}}$  in the  $q = 0$  collective mode, which is of the order of the consequent magneto-crystalline anisotropy energy per atom –  $K \approx 0.1$  meV in Cobalt[8] – and to introduce the possibility of decay of long-wavelength collective excitations into particle-hole excitations[9, 10], a process that contributes substantially to the collective excitation lifetime[30] for the case of NiFe thin films. In the absence of spin-orbit interactions, the ferromagnetic resonance is coupled only to spin-flip particle-hole excitations which at long wavelengths have a gap of the order of the spin-splitting field  $\Delta$ . Gapless spin-flip particle-hole excitations are possible only at wavevectors exceeding the minimum  $q$ -space separation between majority and minority spin Fermi surfaces. The separation in energy at long-wavelengths between collective modes and spin-flip particle-hole continuum implies that low-energy collective modes are only weakly damped. Beyond a critical value of  $q$  the spin-wave branch merges with the continuum. Thus spin-waves can decay into Stoner excitations. The strength of this decay process is sensitive to the character of the orbitals involved in the particle-hole excitations[11]. In the present work we will focus on how this description of elementary spin excitations in itinerant ferromagnets has to be altered when the level spacing for quasi-particle excitations  $\delta$  is finite and approaches  $E_{\text{res}}$ , a condition that is satisfied in the nanometer particle-size range. Note that  $\delta$  is inversely proportional to particle volume, while  $E_{\text{res}}$  is approximately volume independent for large nanoparticles. Since in a finite system there is no wavevector conservation, collective modes and spin-flip particle-hole pairs cannot be simply separated, unlike the bulk case. We will show that this fact, together with the essential role played by spin-orbit interaction, has profound consequences on the nature of the elementary spin excitations in ferromagnetic metal nanoparticles.

The paper is organized in the following way. In Sec. II we introduce two similar microscopic models for a magnetic metal nanoparticle and explain how they are related to the phenomenological model considered previously. The models differ in that one accounts for the difference in the strength of exchange interactions between s and d electrons in transition metals, a feature whose consequences we wish to address specifically. In Sec. III we derive a path integral formulation of theories based on these models[12]. This point of view provides a convenient language for explaining the interplay between collective modes and particle-hole excitations, and for making contact with classical micromagnetic theory. The spin-orientation fluctuation propagator in the Gaussian approximation is discussed in Sec. IV. The poles of the fluctuation propagator occur at the elementary spin excitations of the system. We will show that the ferro-

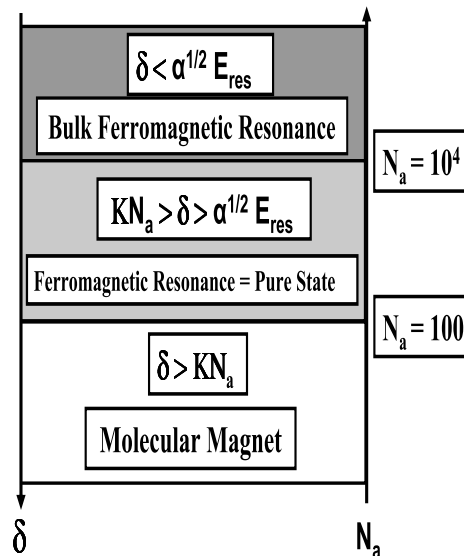


FIG. 1: Crossing of relevant energy scales as a function of the number of atoms  $N_a$  in a magnetic nanoparticle. Here  $\delta$  is the single-particle mean level spacing;  $E_{\text{res}}$  is the energy of the coherent spin collective mode or ferromagnetic resonance energy;  $K$  is the magneto-crystalline anisotropy energy per atom, and  $\alpha$  is the Gilbert damping factor.

magnetic resonance energy  $E_{\text{res}}$  can be expressed as the quotient of anisotropy energy and Berry curvature coefficients which specify the Gaussian expansion of the action at low frequencies. We then discuss how the resonance evolves with particle-size. Our main conclusions is summarized in Fig. 1. For large particle-sizes the ferromagnetic resonance weight is distributed over a large number of particle-hole excitations, while for smaller particle sizes the ferromagnetic resonance appears as a pure quantum excitation. The crossover between the two regimes occurs approximately where the level spacing  $\delta$  is equal to  $\sqrt{\alpha} E_{\text{res}}$  where  $\alpha$  is the bulk resonance's Gilbert damping factor[13]. For typical transition metal nanoparticles this condition is satisfied in particles containing of order  $10^4$  atoms. For smaller particles, avoided crossings between collective and individual particle-hole excitations will occur occasionally as a function of system parameters, for example as a function of an external magnetic field used to reorient the magnetization. For nanoparticles containing fewer than of order  $10^2$  atoms, avoided crossings with particle-hole excitations will usually not occur at any field orientation, and the nanoparticle can be considered to be a molecular magnet in which only spin-orientation degrees of freedom are important at low energies[14]. In Sec. V we will present numerical results for a few-hundred atom nanoparticle, which illustrate some of the these points. Finally in Sec. VI we summarize our findings and comment on their relevance in understanding current tunneling experiments.

## II. QUANTUM MODELS OF A FERROMAGNETIC METAL NANOPARTICLE

In this article we consider two slightly different quantum models chosen to describe both collective and quasiparticle physics in a magnetic metal nanoparticle. We will denote them as Local D-orbital Exchange model (LDE model) and Long-Range Exchange model (LRE model) respectively, for reasons that will become clear below. We will see that these models, when solved within a mean-field approximation, are essentially equivalent and provide a convenient quantum description of a ferromagnetic nanoparticle when the magnetization is *coherent* (spatially constant across the sample). Our use of these models is motivated partly by the evident success of spin-density-functional theory in describing ferromagnetism in transition metals; our formalism could easily be adapted to be compatible with this method of calculating the energies of different magnetic configurations. The models are intended to be sufficiently realistic to capture generic aspects of transition metal nanoparticle magnetism, but evidently miss features that can be important in practice such as variation in exchange interaction strength and inter-atom hopping amplitudes near the surface of the nanoparticle.

### A. Local D-orbital Exchange Model

The first model that we consider accounts qualitatively for the orbital dependence of exchange interaction strengths in a transition metal itinerant-electron ferromagnets [7]. We model the nanoparticle as a cluster of  $\mathcal{N}_a$  atoms located on the sites of a truncated crystal. The numerical results we present here are for a cobalt cluster whose truncated f.c.c. crystal is circumscribed by a hemisphere whose equator lies in the  $XY$ -plane of the f.c.c. crystal[31]. The choice of a hemisphere is motivated by the tunneling experiments of Ref. 2, 3. We use a s-p-d tight-binding model for the quasiparticle orbitals, with 18 orbitals per atom, including the spin-degree of freedom. Nine orbitals per Co atom are occupied in neutral nanoparticles. The full second-quantized Hamiltonian is,

$$\hat{\mathcal{H}} = \hat{H}_{\text{band}} + \hat{H}_{\text{exch}} + \hat{H}_{\text{so}} + \hat{H}_{\text{Zee}}. \quad (1)$$

The second-quantized one-body term

$$\hat{H}_{\text{band}} = \sum_{i,j} \sum_s \sum_{\mu_1, \mu_2} t_{\mu_1, \mu_2, s}^{i,j} c_{i, \mu_1, s}^\dagger c_{j, \mu_2, s} \quad (2)$$

is written in terms of creation and annihilation operators  $c_{i, \mu_1, s}^\dagger$  and  $c_{j, \mu_2, s}$  labeled by atomic-site indexes  $i, j$ , atomic angular momentum indexes  $\mu_1, \mu_2$  and spin indexes  $s, s'$ . We choose the spin-quantization axis to be along the direction of the magnetization, which is specified by a unit vector  $\hat{\Omega}(\Theta, \Phi)$  where  $\Theta$  and  $\Phi$  are the usual angular coordinates defined with respect to the f.c.c. crystal axes. The parameters  $t_{\mu_1, \mu_2, s}^{i,j}$  are Slater-Koster parameters[15] obtained after performing a Löwdin symmetric orthogonalization procedure[16] on the set of Slater-Koster parameters for non-orthogonal atomic orbitals of bulk spin-unpolarized Co[17]. Here the exchange term is a short-range spin-interaction involving only the electrons spins of  $d$ -orbitals on the same atomic site:

$$\hat{H}_{\text{exch}} = -2U_{dd} \sum_i \vec{S}_{d,i} \cdot \vec{S}_{d,i}, \quad (3)$$

where

$$\vec{S}_{d,i} \equiv \sum_{\mu \in d} \vec{S}_{i, \mu} = \sum_{\mu \in d} \frac{1}{2} \sum_{s, s'} c_{i, \mu, s}^\dagger \vec{\sigma}_{s, s'} c_{i, \mu, s'}, \quad (4)$$

$\vec{\sigma}$  being a vector whose components  $\sigma^\alpha$ ,  $\alpha = x, y, z$  are the three Pauli matrices. The parameter  $U_{dd}$  in Eq. (3) determines the strength of the exchange interaction and we will set it equal to 1 eV in our numerical calculations[7]. This choice leads to the correct magnetization per atom in the bulk.

The spin-orbit coupling  $\hat{H}_{\text{so}}$  is a *local* one-body operator

$$\hat{H}_{\text{so}} = \xi_d \sum_i \sum_{\mu, \mu', s, s'} \langle \mu, s | \vec{L} \cdot \vec{S} | \mu', s' \rangle c_{i, \mu, s}^\dagger c_{i, \mu', s'}, \quad (5)$$

where the atomic matrix elements  $\langle \mu, s | \vec{L} \cdot \vec{S} | \mu', s' \rangle \equiv \langle i, \mu, s | \vec{L} \cdot \vec{S} | i, \mu', s' \rangle$  depend on the spin-quantization axis specified by the angles  $\Theta$  and  $\Phi$ . The energy scale  $\xi_d$ , which characterizes the coupling between spin and orbital degrees of freedom, varies in the range from 50 to 100 meV in bulk 3d transition metal ferromagnets[18]. Finally,  $\hat{H}_{\text{Zee}}$  is a local one-body operator describing the Zeeman coupling of the orbital and spin degrees of freedom to an external magnetic field  $\vec{H}_{\text{ext}}$ :

$$\begin{aligned} \hat{H}_{\text{Zee}} &= -\mu_B \sum_i \sum_{\mu, \mu', s, s'} \langle \mu, s | (\vec{L} + g_s \vec{S}) | \mu', s' \rangle \cdot \vec{H}_{\text{ext}} c_{i, \mu, s}^\dagger c_{i, \mu', s'} \\ &= -\mu_B \sum_i \vec{H}_{\text{ext}} \cdot \left\{ \sum_{\mu, \mu', s} \langle \mu, s | \vec{L} | \mu', s \rangle c_{i, \mu, s}^\dagger c_{i, \mu', s} + \frac{g_s}{2} \sum_{\mu, s, s'} c_{i, \mu, s}^\dagger \vec{\sigma}_{s, s'} c_{i, \mu, s'} \right\}, \end{aligned} \quad (6)$$

with  $g_s = 2$ .  $\hat{H}_{Zee}$  plays an important role in manipulating many-body states. In Ref. (7) we have investigated the spectrum of the microscopic Hamiltonian of Eq. (1), treating the quartic exchange interaction in the mean-field approximation. We have focused in particular on the mesoscopic physics of the quasiparticle energies and their complex behavior as a function of the magnetization orientation and external magnetic field orientation and strength. This analysis, although very relevant to the understanding of tunneling experiments, does not tell us anything about the quantization of the collective magnetization orientation dynamics. For this purpose and for the purpose of making a connection with the classical micromagnetic theory, the path integral approach described

in the next section provides a more useful language.

## B. Long-Range Exchange Model

Our microscopic LDE model, when solved in the mean-field approximation, is related to a toy model, originally introduced in Ref. (4), which can be regarded as the simplest possible model of a ferromagnetic metal nanoparticle. The toy model Hamiltonian assumes identical exchange constants between all pairs of single-particle orbitals in the nanoparticle:

$$\hat{\mathcal{H}} = \sum_{n,s} c_{n,s}^\dagger c_{n,s} \epsilon_n - \frac{U}{8\mathcal{N}_a} \sum_{n,m} \sum_{s,s',t,t'} c_{n,s'}^\dagger \vec{\sigma}_{s',s} c_{n,s} \cdot c_{m,t'}^\dagger \vec{\sigma}_{t',t} c_{m,t} = \hat{H}_{\text{band}} - \frac{1}{2} \frac{U}{\mathcal{N}_a} \vec{S} \cdot \vec{S}. \quad (7)$$

In Eq. 7  $c_{n,s}^\dagger$  and  $c_{n,s}$  are Fermion creation and annihilation operators for a quasi-particle state characterized by orbital energy  $\epsilon_n$  and spin component  $s$ ;  $\vec{S} = \frac{1}{2} \sum_n c_{n,s'}^\dagger \vec{\sigma}_{s',s} c_{n,s}$  is the total spin of the nanoparticle. The single particle orbitals will have an average spacing inversely proportional to the volume of the nanoparticle (or the number of atoms  $\mathcal{N}_a$ ) and are expected to exhibit spectral rigidity[19]. The one-body term in this Hamiltonian,  $\hat{H}_{\text{band}}$ , should be thought of as including a mean-field approximation to those spin-independent portions of the interaction not captured by the exchange term  $\hat{H}_{\text{exch}} = -\frac{1}{2} \frac{U}{\mathcal{N}_a} \vec{S} \cdot \vec{S}$ . The many-particle spectrum of this Hamiltonian has been discussed in detail in Ref. (4).

This toy model Hamiltonian can be further augmented[12] by a one-body spin-orbit coupling term  $H_{\text{so}}$ . We can write  $\hat{H}_{\text{so}}$  as[1]

$$\hat{H}_{\text{so}} = \sum_{n,m,s} v_{n,m}^s c_{n,s}^\dagger c_{n,\bar{s}}, \quad (8)$$

with

$$v_{n,m}^s = (v_{n,m}^{\bar{s}})^* = -v_{m,n}^s, \quad v_{n,n}^s = 0, \quad (9)$$

where the conditions on the matrix elements  $v_{n,m}^s$  specified in Eq. (9) ensure that  $\hat{H}_{\text{so}}$  is hermitian and invariant under time-reversal.

Consider the orbital part of the microscopic Hamiltonian given in Eq. (1). Since  $\hat{H}_{\text{band}}$  is quadratic, it can be diagonalized by a canonical transformation:

$$\hat{H}_{\text{band}} = \sum_{i,j} \sum_s \sum_{\mu_1,\mu_2} t_{\mu_1,\mu_2,s}^{i,j} c_{i,\mu_1,s}^\dagger c_{j,\mu_2,s} = \sum_{n,s} c_{n,s}^\dagger c_{n,s} \epsilon_n, \quad (10)$$

where

$$c_{n,s} = \sum_{i,\mu,t} \langle n, s | i, \mu, t \rangle c_{i,\mu,t}, \quad (11)$$

and  $|n, s\rangle$  are the orthonormal eigenvectors. The eigenvalues  $\epsilon_n$  in Eq. (10) can be identified with the doubly degenerate orbital energies of the toy model Hamiltonian in Eq. (7). If we now use Eq. (11) and the completeness of the eigenstates  $\{|i, \mu, t\rangle\}_{i,\mu,t}$ , we can rewrite the exchange interaction of Eq. (7) in the form

$$\hat{H}_{\text{exch}} = -\frac{1}{2} \frac{U}{\mathcal{N}_a} \vec{S} \cdot \vec{S} = -\frac{U}{2\mathcal{N}_a} \frac{1}{4} \sum_{i,j} \vec{S}_i \cdot \vec{S}_j \quad (12)$$

with  $\vec{S}_i \equiv \sum_\mu S_{i\mu}$ . From Eq. (12) it is clear that the toy model Hamiltonian with equal exchange constants is equivalent to a microscopic model with a *long-range exchange* interaction, coupling the spin of each atomic orbital at each atomic site to all others; hence the name of Long-Range Exchange model (LRE model). We emphasize that the electron spins of all orbitals are coupled in this model, not just the spins of  $d$ -orbitals. From Eq. (12) it follows that in a constrained mean-field approximation where the local moment  $\langle \vec{S}_i \rangle$  is forced to be *coherent* across the sample and the spins of *all* atomic orbitals are exchange-coupled, the microscopic LDE model and the the LRE model would be equivalent equivalent, (with  $2U_{dd} \Leftrightarrow U/8$ ). Differences arise when only the the  $d$ -orbitals in the LDE model are exchange-coupled, which we comment on below.

Neither model includes any magnetostatic dipole-dipole interactions, which can be important in some circumstances, for example when the nanoparticle is not close to spherical, but are easily incorporated in our discussion. Note however, that both models lead to strong

shape dependence, because of surface effects which are important when the particle size is small. In Sec. (V) we will see that the structure of particle-hole excitations of the LDE model when only the spins of d-orbitals are coupled is richer than when quasiparticle majority and minority spins are simply shifted by a rigid exchange field, as in the case of the LRE model.

### III. AUXILIARY FIELD FORMULATION

#### A. Coherent state functional integral and Hubbard-Stratonovich transformation

We consider first our LRE toy model. The extension to the LDE model is straightforward and we will comment on it below. Following some familiar steps[20, 21],

we write the interacting fermion partition function as an imaginary time coherent state path integral

$$Z = \int \mathcal{D}[\bar{\psi}(\tau) \psi(\tau)] \exp(-\mathcal{S}), \quad (13)$$

where the action  $\mathcal{S}$  is

$$\mathcal{S} = \int_0^\beta d\tau \left[ \sum_{n,s} \bar{\psi}_{n,s}(\tau) \left( \frac{\partial}{\partial \tau} - \mu \right) \psi_{n,s}(\tau) + \mathcal{H}(\bar{\psi}(\tau), \psi(\tau)) \right]. \quad (14)$$

Here  $\beta = 1/k_B T$ ,  $\mu$  is the chemical potential and we use units such that  $\hbar = 1$ . Since the exchange interaction term in our toy model is quadratic in the total electron spin – see Eq. (7) – its contribution to the action for each time step  $\tau_k = k\epsilon = k\beta/N$  can be represented by a Gaussian integral over a real vector field  $\vec{\Delta}_k \equiv \vec{\Delta}(\tau_k)$

$$\int d\vec{\Delta}_k e^{-\frac{N\epsilon}{2U} \vec{\Delta}_k \cdot \vec{\Delta}_k + \vec{\Delta}_k \cdot \frac{1}{2} \sum_{n,s,s'} \bar{\psi}_{n,s}(\tau_k) \vec{\sigma}_{s,s'} \psi_{n,s'}(\tau_{k-1})} \propto e^{-H_{\text{exch}}(\bar{\psi}(\tau_k), \psi(\tau_{k-1}))}. \quad (15)$$

Using this transformation for each time step, we obtain the following functional integral over a single auxiliary field  $\vec{\Delta}(\tau)$  that fluctuates in imaginary time

$$Z = \int \mathcal{D}[\bar{\psi}(\tau) \psi(\tau)] \int \mathcal{D}[\vec{\Delta}(\tau)] \exp(-\mathcal{S}), \quad (16)$$

where the action  $\mathcal{S}$  is

$$\begin{aligned} \mathcal{S} = \int_0^\beta d\tau & \left[ \frac{N_a}{2U} \vec{\Delta}(\tau) \cdot \vec{\Delta}(\tau) + \sum_{n,s} \bar{\psi}_{n,s}(\tau) \left( \frac{\partial}{\partial \tau} - \mu \right) \psi_{n,s}(\tau) + H_{\text{band}}(\bar{\psi}(\tau), \psi(\tau)) \right. \\ & \left. + H_{\text{so}}(\bar{\psi}(\tau), \psi(\tau)) - \frac{1}{2} (\vec{\Delta}(\tau) + g_s \mu_B \vec{H}_{\text{ext}}) \cdot \sum_{n,s} \bar{\psi}_{n,s}(\tau) \vec{\sigma}_{s,s'} \psi_{n,s}(\tau) \right]. \end{aligned} \quad (17)$$

This action can be written in another form which is especially useful for small nanoparticles at low temperatures. Let us consider the fluctuating one-body Hamiltonian

$$\hat{H}_{1b}(\vec{\Delta}(\tau)) = \hat{H}_{\text{band}} + \hat{H}_{\text{so}} - \frac{1}{2} (\vec{\Delta}(\tau) + g_s \mu_B \vec{H}_{\text{ext}}) \cdot \sum_{n,s} c_{n,s}^\dagger \vec{\sigma}_{s'} c_{n,s}. \quad (18)$$

In Eq. (16) we can replace the functional integral over the fermionic coherent states  $\bar{\psi}(\tau), \psi(\tau)$  by a trace of the operator

$$\exp \left( - \int_0^\beta d\tau \hat{H}_{1b}(\vec{\Delta}(\tau)) \right) = \exp \left( - \epsilon \sum_k \hat{H}_{1b}(\vec{\Delta}_k) \right) = \prod_k \exp \left( - \epsilon \hat{H}_{1b}(\vec{\Delta}_k) \right). \quad (19)$$

By inserting at each time step  $\tau_k$  the resolution of the identity  $\hat{I} = \sum_a |\Psi_a(\vec{\Delta}_k)\rangle \langle \Psi_a(\vec{\Delta}_k)|$ , where  $\{|\Psi_a(\vec{\Delta}_k)\rangle\}_a$  is a complete set of eigenstates of the one-body Hamiltonian  $\hat{H}_{1b}(\vec{\Delta}_k)$ , and taking the  $T \rightarrow 0$  limit, we obtain  $Z = \int \mathcal{D}[\vec{\Delta}(\tau)] \exp(-\mathcal{S})$ , with

$$\begin{aligned} \mathcal{S} = & \epsilon \sum_k \frac{N_a}{2U} \vec{\Delta}_k \cdot \vec{\Delta}_k - \ln \left[ \langle \Psi_0(\vec{\Delta}_N) | \exp \left( - \epsilon \hat{H}_{1b}(\vec{\Delta}_{N-1}) \right) | \Psi_0(\vec{\Delta}_{N-1}) \rangle \right. \\ & \left. \times \dots \times \langle \Psi_0(\vec{\Delta}_1) | \exp \left( - \epsilon \hat{H}_{1b}(\vec{\Delta}_N) \right) | \Psi_0(\vec{\Delta}_N) \rangle \right]. \end{aligned} \quad (20)$$

Note that the fluctuating field  $\vec{\Delta}(\tau)$  is bosonic and satisfies periodic boundary conditions  $\vec{\Delta}(0) = \vec{\Delta}(\beta)$ . Since  $\epsilon \rightarrow 0$  we can rewrite the action in the form

$$\mathcal{S} = \int_0^\infty d\tau \left\{ \frac{\mathcal{N}_a}{2U} \vec{\Delta}(\tau) \cdot \vec{\Delta}(\tau) - \frac{1}{\epsilon} \left[ \langle \Psi_0(\vec{\Delta}(\tau + \epsilon)) | e^{-\epsilon \hat{H}_{1b}(\vec{\Delta}(\tau))} | \Psi_0(\vec{\Delta}(\tau)) \rangle - 1 \right] \right\} \quad (21)$$

$$= \int_0^\infty d\tau \left[ \frac{\mathcal{N}_a}{2U} \vec{\Delta}(\tau) \cdot \vec{\Delta}(\tau) + E_{1b}(\vec{\Delta}(\tau)) + \langle \Psi_0 | \partial \Psi_0 / \partial \vec{\Delta} \rangle \cdot \frac{\partial \vec{\Delta}(\tau)}{\partial \tau} \right]. \quad (22)$$

Here  $E_{1b}(\vec{\Delta}(\tau))$  is the ground-state energy of  $\hat{H}_{1b}(\vec{\Delta}(\tau))$ . The approximations that are implicit in these manipulations are valid when collective fluctuations of the spin-splitting field are not strongly coupled to particle-hole excitations.

Eq. (22) will play a crucial role in this paper. The quantity:

$$E_{\text{tot}}[\vec{\Delta}(\tau)] \equiv \frac{\mathcal{N}_a}{2U} \vec{\Delta}(\tau) \cdot \vec{\Delta}(\tau) + E_{1b}(\vec{\Delta}(\tau)), \quad (23)$$

gives the quantum energy functional of the magnetic nanoparticle as a function of the fluctuating spin-splitting field  $\vec{\Delta}(\tau)$ ; its classical limit, obtained by evaluating at zero frequency (i.e. static  $\vec{\Delta}$  independent of time)  $E_{\text{tot}}[\vec{\Delta}(\tau)]$ , corresponds to the phenomenological micro-magnetic energy functional for a coherent magnetic particle with magnetostatic contributions neglected.

The last term in the action

$$\mathcal{S}_{\text{Berry}} \equiv \int_0^\infty d\tau \langle \Psi_0 | \partial \Psi_0 / \partial \vec{\Delta} \rangle \cdot \frac{\partial \vec{\Delta}(\tau)}{\partial \tau}, \quad (24)$$

is a Berry phase term, which is related to the reduction of the total spin component along the magnetization axis due to spin deviations from the ground state configuration[22, 23]. As we will see in Sec. (IV), the Berry phase contribution to the action captures the quantization condition of the collective elementary excitations and the way in which spin-orbit interactions affect this quantization condition.

The Hubbard-Stratonovich decoupling can also be carried out in the case of the LDE model of Eq. 3. Here we should in principle introduce an auxiliary field  $\vec{\Delta}_{d,i}(\tau)$  that is dependent on the atomic site  $i$ . Complicated inhomogeneous and noncollinear spin-splitting fields can indeed occur for very small nanoparticles with a few tens of atoms[24, 25]. In this paper however, we will consider only a *coherent i.e.* site-independent spin-splitting field, which is a good approximation for the relatively large nanoparticles ( $\mathcal{N}_a > 50$ ) that we are interested in.

## B. Mean-Field Approximation

The mean-field approximation for the action is obtained by finding the value of the spin-splitting field at which it is minimized. Since the minimum occurs for

a time-independent spin-splitting field  $\vec{\Delta}_{\text{MF}}$ , the Berry phase contribution to the action does not enter at this level. In the coherent-field approximation, the mean-field spin-splitting satisfies:

$$\begin{aligned} & \frac{\mathcal{N}_a}{U} \vec{\Delta}_{\text{MF}} + \frac{\partial E_{1b}(\vec{\Delta})}{\partial \vec{\Delta}} \Big|_{\vec{\Delta}_{\text{MF}}} \\ &= \frac{\mathcal{N}_a}{U} \vec{\Delta}_{\text{MF}} - \langle \Psi_{\text{MF}} | \vec{S}_{\text{tot}} | \Psi_{\text{MF}} \rangle = 0, \end{aligned} \quad (25)$$

where  $|\Psi_{\text{MF}}\rangle \equiv |\Psi_0(\vec{\Delta}_{\text{MF}})\rangle$ .  $\vec{\Delta}_{\text{MF}}$  may be determined either by minimizing the energy functional or by solving the self-consistent-field equations implied by the second form of Eq.( 25). The same set of mean-field equations can be derived directly from the more general expression for the action in which the functional integral over fermion Grassmann variables is still present[21].

## IV. GAUSSIAN FLUCTUATIONS

Our theory of elementary magnetic excitations of metallic nanoparticles is based on a Gaussian fluctuation theory in which the action is expanded to second order around the static mean-field values of the auxiliary fields. It will prove informative to contrast two approaches that can be used to evaluate the Gaussian fluctuation action. In the first approximation we work directly with the Berry phase and energy terms in the action, which are rather transparently related to micromagnetic theory and Landau-Lifshitz semi-classical dynamics. This approach cannot, however, deal directly with the coupling of collective and particle-hole elementary excitations. In the second approach we expand the action to second order around  $\Delta_{\text{MF}}$ , without introducing the quasi-static energy functional as an intermediate step. We will see that the two approaches are equivalent in the limit of energies smaller than the minimum particle-hole excitation energy.

### A. Energy Functional Approach

If we are interested only in low-energy excitations, which have slow dependence on imaginary time, we can approximate the energy function by its dependence on

static field variations:

$$E_{\text{tot}}(\vec{\Delta}) = E_{\text{MF}} + \frac{1}{2} \tilde{\Delta}^\alpha \left[ \frac{\mathcal{N}_a \delta_{\alpha,\beta}}{U} + \frac{\partial^2 E_{1b}(\vec{\Delta})}{\partial \Delta^\alpha \partial \Delta^\beta} \right]_{\vec{\Delta}_{\text{MF}}} \tilde{\Delta}^\beta, \quad (26)$$

where  $\tilde{\Delta}^\alpha \equiv \Delta^\alpha - \Delta_{\text{MF}}^\alpha$ , and  $E_{\text{MF}} \equiv E_{\text{tot}}(\vec{\Delta}_{\text{MF}})$ . Since amplitude variations are energetically more costly, the dominant fluctuations of the order parameter will be rotations. The second derivative represents the expansion of the micromagnetic energy around its extremum; the dependence of energy on orientation is generally referred to as the anisotropy energy of the nanoparticle.

The bosonic field  $\tilde{\Delta}(\tau)$  is periodic in  $[0, \beta]$ . Therefore the Berry phase contribution to the action given in Eq. (24) can be rewritten as the closed line integral that is path-dependent but not dynamics dependent:

$$\mathcal{S}_{\text{Berry}} = \oint d\vec{\Delta} \cdot \langle \Psi_0 | \partial \Psi_0 / \partial \vec{\Delta} \rangle. \quad (27)$$

Since

$$\begin{aligned} \langle \Psi_0 | \frac{\partial}{\partial \vec{\Delta}} \Psi_0 \rangle + \langle \Psi_0 | \frac{\partial}{\partial \vec{\Delta}} \Psi_0 \rangle^* &= \langle \Psi_0 | \frac{\partial}{\partial \vec{\Delta}} \Psi_0 \rangle + \langle \frac{\partial}{\partial \vec{\Delta}} \Psi_0 | \Psi_0 \rangle \\ &= \frac{\partial}{\partial \vec{\Delta}} \langle \Psi_0 | \Psi_0 \rangle = 0, \end{aligned} \quad (28)$$

the Berry phase  $\mathcal{S}_{\text{Berry}}$  is pure imaginary. For small amplitude rotations around the direction of  $\Delta_{\text{MF}}$ , the closed line integral Eq. (27) is equal to the product of the area of the enclosed path and the Berry curvature,

$$\mathcal{C}(\Delta_{\text{MF}}) = \hat{z} \cdot \vec{\nabla} \times \langle \Psi_0 | \frac{\partial \Psi_0}{\partial \vec{\Delta}} \rangle = \langle \frac{\partial \Psi_0}{\partial \Delta^x} | \frac{\partial \Psi_0}{\partial \Delta^y} \rangle - \langle \frac{\partial \Psi_0}{\partial \Delta^y} | \frac{\partial \Psi_0}{\partial \Delta^x} \rangle. \quad (29)$$

Unlike the integrand of Eq. (27), the Berry curvature is gauge independent, *i.e.* it is independent of the arbitrary phase choice made for the many-electron wavefunction at each magnetization orientation. For small fluctuations the integrand in Eq. (27) can be chosen to be anything whose curl is the constant  $\mathcal{C}(\Delta_{\text{MF}})\hat{z}$ . For example one convenient choice, analogous to the symmetric gauge choice for a constant magnetic field, leads to

$$\mathcal{S}_{\text{Berry}} = \frac{\mathcal{C}(\Delta_{\text{MF}})}{2} \oint [\hat{z} \times \vec{\Delta}] \cdot d\vec{\Delta}, \quad (30)$$

if we choose the  $\hat{z}$  direction to be the direction of  $\vec{\Delta}_{\text{MF}}$ . This line integral can be parametrized in terms of the

imaginary time variable

$$\mathcal{S}_{\text{Berry}} = \frac{\mathcal{C}(\Delta_{\text{MF}})}{2} \int_0^\beta d\tau [\tilde{\Delta}^x \partial_\tau \tilde{\Delta}^y - \tilde{\Delta}^y \partial_\tau \tilde{\Delta}^x], \quad (31)$$

which can also be written in frequency space as

$$\mathcal{S}_{\text{Berry}} = \frac{1}{2\beta} \sum_{i\omega_n} i\omega_n \mathcal{C}(\Delta_{\text{MF}}) [\tilde{\Delta}^x(-i\omega_n) \tilde{\Delta}^y(i\omega_n) - \tilde{\Delta}^y(-i\omega_n) \tilde{\Delta}^x(i\omega_n)]. \quad (32)$$

Eq. (32) shows that the Berry phase contributes a term linear in frequency  $\omega_n$  to the imaginary part of the quadratic Gaussian fluctuation action. We will see that in the next section that the same contribution to the action arises from a small frequency expansion of the spin-fluctuation propagator kernel, defined in the next section.

### 1. Calculation of the Berry's curvature

We now briefly discuss the numerical evaluation of Berry curvatures [22] evaluated at the mean-field-solution point. We start from the expression for  $\mathcal{S}_{\text{Berry}}$  given by Eq. (27), and consider paths on the unit sphere of exchange-field orientations. A small area closed path centered on the mean-field orientation encloses a small area on the unit sphere whose normal is the direction of  $\Delta_{\text{MF}}$ , which we take as the  $\hat{z}$  direction. Using Stoke's theorem and taking the Berry curvature out of the surface integral, we obtain

$$\mathcal{S}_{\text{Berry}} = \mathcal{C}(\Delta_{\text{MF}}) \int_{\text{Area}} dS_\Delta, \quad (33)$$

For our calculation we consider as a closed path a small right triangle in the  $xy$ -plane of sides  $\Delta_x = \Delta_y = \Delta_{\text{MF}}\theta$ , where  $\theta$  is a small angle describing the rotation around the  $x$  and  $y$  axis. Then

$$\mathcal{S}_{\text{Berry}} = \frac{1}{2} \mathcal{C}(\Delta_{\text{MF}}) \Delta_{\text{MF}}^2 \theta^2. \quad (34)$$

This Berry phase can also be expressed as [22]

$$i\mathcal{S}_{\text{Berry}} = -\text{Im} \ln \left[ \langle \Psi_{\text{MF}} | \Psi_0(\vec{\Delta}_x) \rangle \langle \Psi_0(\vec{\Delta}_x) | \Psi_0(\vec{\Delta}_y) \rangle \langle \Psi_0(\vec{\Delta}_y) | \Psi_{\text{MF}} \rangle \right], \quad (35)$$

where  $|\Psi_0(\vec{\Delta}_x)\rangle$  and  $|\Psi_0(\vec{\Delta}_y)\rangle$  are the single Slater deter-

minants of lowest energy for exchange fields that differ

from the mean-field value by  $\Delta_x \hat{x}$ , and  $\Delta_y \hat{y}$  respectively. Eq. (34) can be obtained by expanding  $|\Psi_0(\vec{\Delta}_x)\rangle$  and  $|\Psi_0(\vec{\Delta}_y)\rangle$  to quadratic order in  $\Delta_x$  and  $\Delta_y$ , remembering that  $\langle\Psi_0|\frac{\partial}{\partial\vec{\Delta}}\Psi_0\rangle$  is pure imaginary. The expression for the Berry phase given in Eq. (34) is very suitable for numerical calculations, since the wavefunctions  $|\Psi_0(\vec{\Delta}_x)\rangle$  and  $|\Psi_0(\vec{\Delta}_y)\rangle$  can be easily calculated. The arbitrary phases of the wave functions at the three vertices explicitly cancel since each wave function *and* its complex conjugate appears in Eq. (34). If we choose the arbitrary phases in such a way that the matrix elements of  $|\Psi_0(\vec{\Delta}_x)\rangle$  and  $|\Psi_0(\vec{\Delta}_y)\rangle$  with  $|\Psi_{\text{MF}}\rangle$  are real and positive, then the Berry phase is given by the simplified expression

$$i\mathcal{S}_{\text{Berry}} = \text{Im} \ln \langle\Psi_0(\vec{\Delta}_x)|\Psi_0(\vec{\Delta}_y)\rangle. \quad (36)$$

Finally, one can show that the Berry phase (or Berry curvature) of the many-body wave function is given by the sum of the Berry phases (or curvatures) of the occupied single particle states, even in the presence of spin-orbit interaction. The easiest way to prove this is to show that

$$\langle\Psi_0|\frac{\partial}{\partial\vec{\Delta}}\Psi_0\rangle = \sum_n^{\text{occ}} \langle\phi_n|\frac{\partial}{\partial\vec{\Delta}}\phi_n\rangle, \quad (37)$$

where  $\phi_n$  are single-particle eigenstates of the one-body Hamiltonian. The gradient in Eq. (37) acts separately on the single-particle wave functions and hence it can be regarded as a sum of single-particle operators. It follows that the Berry phase can be expressed as

$$i\mathcal{S}_{\text{Berry}} = \sum_n^{\text{occ}} \text{Im} \ln \langle\phi_n(\vec{\Delta}_x)|\phi_n(\vec{\Delta}_y)\rangle. \quad (38)$$

## 2. Berry phase without spin-orbit coupling

For the case of no spin-orbit coupling, the Berry phase term can be calculated analytically and is equal to the number of singly-occupied orbitals times the usual spin-1/2 Berry phase. To show this, let us consider a many-body wave-function within the long-range exchange model describing a state polarized in the direction  $\hat{\Omega} \equiv \vec{\Delta}/\Delta$

$$|\Psi_0(\vec{\Delta})\rangle = \prod_s (u(\hat{\Omega})c_{s\uparrow}^\dagger + v(\hat{\Omega})c_{s\downarrow}^\dagger) \prod_d c_{d\uparrow}^\dagger c_{d\downarrow}^\dagger |0\rangle \equiv |\Psi_0(\hat{\Omega})\rangle, \quad (39)$$

where the index  $s$  runs over the  $N_\uparrow - N_\downarrow$  singly-occupied states and the index  $d$  over the  $N_\downarrow$  doubly-occupied states. The functions  $u(\hat{\Omega})$  and  $v(\hat{\Omega})$  are written in terms of the angles  $\Theta$  and  $\Phi$  specifying the unit vector  $\hat{\Omega}(\Theta, \Phi)$

$$u(\hat{\Omega}) = \cos(\Theta/2), \quad (40)$$

$$v(\hat{\Omega}) = e^{i\Phi} \sin(\Theta/2). \quad (41)$$

We obtain

$$\begin{aligned} \left|\frac{\partial\Psi_0(\hat{\Omega})}{\partial\hat{\Omega}}\right\rangle &= \sum_s \left(\frac{\partial u}{\partial\hat{\Omega}}c_{s\uparrow}^\dagger + \frac{\partial v}{\partial\hat{\Omega}}c_{s\downarrow}^\dagger\right) \\ &\times \prod_{s' \neq s} (u(\hat{\Omega})c_{s'\uparrow}^\dagger + v(\hat{\Omega})c_{s'\downarrow}^\dagger) \prod_d c_{d\uparrow}^\dagger c_{d\downarrow}^\dagger |0\rangle. \end{aligned} \quad (42)$$

Hence, for rotations of the spin-splitting field

$$\begin{aligned} \langle\Psi_0|\frac{\partial\Psi_0}{\partial\vec{\Delta}}\rangle &= \langle\Psi_0|\frac{\partial\Psi_0}{\partial\hat{\Omega}}\rangle = \sum_s (u^* \frac{\partial u}{\partial\hat{\Omega}} + v^* \frac{\partial v}{\partial\hat{\Omega}}) \\ &= \sum_s i \frac{1 - \cos(\Theta)}{2 \sin(\Theta)} \hat{\Phi} = i \frac{N_\uparrow - N_\downarrow}{2} \frac{1 - \cos(\Theta)}{\sin(\Theta)} \hat{\Phi} \end{aligned} \quad (43)$$

and the Berry phase

$$\begin{aligned} \mathcal{S}_{\text{Berry}} &= \int_0^\beta d\tau \langle\Psi_0|\frac{\partial\Psi_0}{\partial\hat{\Omega}}\rangle \cdot \frac{d\hat{\Omega}}{d\tau} = \oint \langle\Psi_0|\frac{\partial\Psi_0}{\partial\hat{\Omega}}\rangle \cdot d\hat{\Omega} \\ &= i \frac{N_\uparrow - N_\downarrow}{2} \oint d\Phi (1 - \cos(\Theta_\Phi)) \\ &= i [N_\uparrow - N_\downarrow] \frac{A[\hat{\Omega}]}{2}, \end{aligned} \quad (44)$$

where  $A[\hat{\Omega}]$  is the area enclosed by the path  $\Omega(\tau)$  on the unit sphere, and  $A[\hat{\Omega}]/2$  is the usual spin-1/2 Berry phase. In the presence of spin-orbit interactions, the Berry phase becomes highly non-trivial as we discuss in Sec.V.

For a path enclosing the small right triangle described in Sec. IV A 1,  $A[\hat{\Omega}] = \theta^2/2$  and

$$\mathcal{S}_{\text{Berry}} = i \frac{\theta^2 S}{2}, \quad (45)$$

$$\mathcal{C}(\Delta_{\text{MF}}) = i \frac{S}{\Delta_{\text{MF}}^2}, \quad (46)$$

where  $S = (N_\uparrow - N_\downarrow)/2$  is the total spin in the nanoparticle ground state.

## B. Gaussian Fluctuations: Perturbation Theory Approach

The Gaussian fluctuations theory can be derived more generally by formally integrating out the fermions and then expanding second order around  $\Delta_{\text{MF}}$  without making any quasi-static approximations. We discuss the case of the long-range exchange interaction first and then indicate what changes occur in the short-range (d-only) exchange model. The formally exact expression for the action is

$$S = \int_0^\beta \frac{N_a}{2U} \vec{\Delta} \cdot \vec{\Delta} - \ln \det(\partial_\tau + H_{1b}(\Delta_{\text{MF}}^\alpha + \vec{\Delta}^\alpha)). \quad (47)$$

where  $H_{1b}(\Delta)$  includes, in addition to its single-particle hopping and spin-orbit terms, the spin splitting terms



$-(\vec{\Delta}_{\text{MF}} + \vec{H}_{\text{ext}}) \cdot \vec{s} + \tilde{\Delta}^\alpha s^\alpha$ . It is the second of these two terms that is treated perturbatively. First order terms in the expansion vanish, since the mean-field value of  $\vec{\Delta}$  is an extremum of the action. The second order terms can be obtained by a standard calculation with the following result:

$$\mathcal{S}_{\text{fluc}} = \frac{1}{2\beta} \sum_{i\omega_n} \tilde{\Delta}^\beta(-i\omega_n) K_{\beta\alpha}(i\omega_n) \tilde{\Delta}^\alpha(i\omega_n), \quad (48)$$

where the kernel  $K_{\beta\alpha}(i\omega_n)$  is the inverse of the exchange-field-fluctuation propagator and is given by

$$K_{\beta\alpha}(i\omega_n) = \delta_{\alpha,\beta} \frac{\mathcal{N}_a}{U} + \sum_{I,J} \frac{n_F(\xi_J) - n_F(\xi_I)}{i\omega_n + \xi_J - \xi_I} \times \langle J | s^\beta | I \rangle \langle I | s^\alpha | J \rangle \quad (49)$$

where  $|I\rangle$  is a mean-field electron eigenstate and  $\xi_I$  is the corresponding eigenvalue with energies measured from the chemical potential.

Fluctuations in the magnetization orientation around the mean field direction  $\hat{z} = \vec{\Delta}_{\text{MF}}/\Delta_{\text{MF}}$ , are described by the transverse diagonal  $K_{xx}$ ,  $K_{yy}$  and off-diagonal  $K_{xy}$ ,  $K_{yx}$  components of the kernel. It is customary to introduce  $K_{+-}(i\omega_n)$  and  $K_{-+}(i\omega_n)$ . When the spin-orbit interaction is present,  $K_{++}(i\omega_n)$  and  $K_{--}(i\omega_n)$  do not vanish and play a role. Note that

$$K_{-+}(i\omega_n) = K_{+-}(-i\omega_n), \quad (50)$$

$$K_{++}(-i\omega_n) = K_{++}(i\omega_n), \quad (51)$$

$$K_{--}(i\omega_n) = K_{++}(-i\omega_n)^*. \quad (52)$$

It follows from Eq. (49) that

$$K_{xx} = \mathcal{N}_a/U + (K_{+-} + K_{-+})/4 + (K_{++} + K_{--})/4, \quad (53)$$

$$K_{yy} = \mathcal{N}_a/U + (K_{+-} + K_{-+})/4 - (K_{++} + K_{--})/4, \quad (54)$$

$$K_{xy} = i(K_{+-} - K_{-+})/4 - i(K_{++} - K_{--})/4, \quad (55)$$

and

$$K_{yx} = -i(K_{+-} - K_{-+})/4 - i(K_{++} - K_{--})/4. \quad (56)$$

The transverse fluctuation action of the long-range exchange model is quite simple in the absence of spin-orbit interactions. Firstly, the components  $K_{++} = K_{--} = 0$ , since the spin of the quasi-particle states is a good quantum number. (This property depends only on spin-rotational invariance and holds for the short-range exchange model as well). Furthermore, since the the electron mean-field eigenstates factorize into spin and orbital

factors identical spin-up and spin-down wavefunctions are split energetically by  $\Delta_{\text{MF}}$  and we obtain

$$K_{+-}(i\omega_n) = \frac{N_\uparrow - N_\downarrow}{i\omega_n - (\Delta_{\text{MF}} + H_{\text{ext}})} = K_{-+}(-i\omega_n). \quad (57)$$

In examining the consequences of this simple property for the Gaussian action kernel, we first consider  $K_{xy}(i\omega_n)$ . We see from Eq. (57) that when there is no spin-orbit interaction,  $K_{xy}(i\omega_n = 0) = 0$ , a property that reflects invariance under rotations of exchange-field orientation around the  $\hat{z}$  axis. By expanding  $K_{xy}(i\omega_n)$  around  $i\omega_n = 0$ , we obtain

$$K_{xy}(i\omega_n) \approx -i\omega_n i \frac{N_\uparrow - N_\downarrow}{2\Delta_{\text{MF}}^2} = -\frac{iS}{\Delta_{\text{MF}}^2} i\omega_n. \quad (58)$$

By inserting Eq. (58) into Eq. (48) and comparing the result with Eq. (32), we can identify the term of  $K_{xy}(i\omega_n)$  linear in  $i\omega_n$ ,  $iS/\Delta_{\text{MF}}^2$ , with the Berry curvature,  $\mathcal{C}(\Delta_{\text{MF}})$ , in agreement with Eq. (46).

Similarly, the expansion of  $K_{xx}(i\omega_n) = K_{yy}(i\omega_n)$  around  $i\omega_n = 0$  yields

$$\begin{aligned} K_{xx}(i\omega_n) = K_{yy}(i\omega_n) &\approx \frac{\mathcal{N}_a}{U} - \frac{N_\uparrow - N_\downarrow}{2\Delta_{\text{MF}}} + \mathcal{O}(\omega_n^2) \\ &= 0 + \mathcal{O}(\omega_n^2), \end{aligned} \quad (59)$$

where in the last equality of Eq. (59) we have used the mean-field relationship  $(U/\mathcal{N}_a)S = \Delta_{\text{MF}}$  between the total magnetization of the nanoparticle and the spin-splitting field. The vanishing of the diagonal components  $K_{xx}$  and  $K_{yy}$  at  $\omega_n = 0$  is again a result of rotational invariance. In the absence of spin-orbit interactions there is a collective mode at zero energy because of magnetization-orientation rotational invariance.

The physics that we wish to investigate in this paper is largely contained in the way that the simple results outlined above are altered by spin-orbit interactions. As we have stated, both Berry-phase and the energy-term in the action become highly non-trivial, a property that we now examine from the perturbation theory point-of-view. From Eqs. (50)-(56) it is clear that  $K_{xx}(\omega_n)$ ,  $K_{yy}(\omega_n)$ ,  $K_{xy}(\omega_n)$  and  $K_{yx}(\omega)$  are real at  $\omega_n = 0$ . Comparing Eq. (26) with the  $\omega_n = 0$  term of Eq. (48), we see that the kernel coefficients reduce to the time-independent perturbation theory expressions for the second derivatives of the total energy with respect to exchange field,  $\partial^2 E_{\text{tot}}(\vec{\Delta}_{\text{MF}})/\partial\Delta^x \partial\Delta^x$ ,  $\partial^2 E_{\text{tot}}(\vec{\Delta}_{\text{MF}})/\Delta^y \partial\Delta^y$ . In its static limit, the fluctuation kernel reduces to one that would be obtained from a classical theory with the micromagnetic energy functional derived from a mean-field-theory calculation, or for accurate first principles calculations by solving spin-density-functional Kohn Sham equations self-consistently. By expanding  $K_{\alpha\beta}(i\omega_n)$  around  $i\omega_n = 0$ , we obtain

$$K_{xx}(i\omega_n) \approx \frac{\partial^2 E_{\text{tot}}(\vec{\Delta}_{\text{MF}})}{\partial \Delta^x \partial \Delta^x} + \mathcal{O}(\omega_n^2) = (a + b) + \mathcal{O}(\omega_n^2), \quad (60)$$

$$K_{yy}(i\omega_n) \approx \frac{\partial^2 E_{\text{tot}}(\vec{\Delta}_{\text{MF}})}{\partial \Delta^y \partial \Delta^y} + \mathcal{O}(\omega_n^2) = (a - b) + \mathcal{O}(\omega_n^2), \quad (61)$$

$$K_{xy}(i\omega_n) \approx \frac{\partial^2 E_{\text{tot}}(\vec{\Delta}_{\text{MF}})}{\partial \Delta^x \partial \Delta^y} - \mathcal{C}(\Delta_{\text{MF}}) i\omega_n = c - \mathcal{C}(\Delta_{\text{MF}}) i\omega_n, \quad (62)$$

$$K_{yx}(i\omega_n) \approx \frac{\partial^2 E_{\text{tot}}(\vec{\Delta}_{\text{MF}})}{\partial \Delta^y \partial \Delta^x} + \mathcal{C}(\Delta_{\text{MF}}) i\omega_n = c + \mathcal{C}(\Delta_{\text{MF}}) i\omega_n, \quad (63)$$

where

$$a = \frac{\mathcal{N}_a}{U} + \frac{K_{+-}(0)}{2}, \quad (64)$$

$$b = \frac{K_{++}(0) + K_{++}(0)^*}{4}, \quad (65)$$

$$c = -i \frac{K_{++}(0) - K_{++}(0)^*}{4}, \quad (66)$$

are real constants and the Berry curvature is

$$\mathcal{C}(\Delta_{\text{MF}}) = \frac{i}{2} \sum_{I,J} \frac{n_F(\xi_J) - n_F(\xi_I)}{(\xi_J - \xi_I)^2} |\langle J|s^+|I\rangle|^2. \quad (67)$$

This expression for the Berry curvature can also be derived from Eq.( 29) by using time-independent perturbation theory expressions for the dependence of single-particle wavefunctions on exchange-field orientation. Note that the leading frequency dependences in  $K_{xx}$  and  $K_{yy}$  are quadratic. These equations are valid for  $i\omega_n$  smaller than the smallest particle-hole excitation energy  $|\xi_J - \xi_I|$ , as we discuss at greater length below. So far we have completely disregarded amplitude fluctuations of the exchange field, *i.e.* the components of the Kernel involving  $\Delta^z$ . It is obvious that in absence of spin-orbit interactions

$$K_{xz}(i\omega_n) = K_{zx}(i\omega_n) = 0, \quad (68)$$

$$K_{yz}(i\omega_n) = K_{zy}(i\omega_n) = 0, \quad (69)$$

$$K_{zz}(i\omega_n) = \frac{\mathcal{N}_a}{U} + \frac{\delta_{n,0}}{4} \sum_I \frac{\partial n_F}{\partial \xi} \Big|_{\xi=\xi_I}. \quad (70)$$

When spin-orbit is present, the off-diagonal components involving  $\Delta^z$  are in principle non-zero. However it turns out that they are always very small (see next section); therefore we will typically neglect them and we will only keep  $K_{zz}(i\omega_n) = \mathcal{N}_a/U$ . This approximation amounts to neglecting the weak dependence of the magnitude of the exchange field on its orientation.

### C. Excitation Spectrum

The kernel of the fluctuation action is the *matrix inverse* of the exchange-field propagator, which is proportional to the spin susceptibility linear response function. We refer to this propagator below as the spin-susceptibility.

$$\chi_{\alpha\beta}(i\omega_n) = [K(i\omega_n)^{-1}]_{\alpha\beta} \quad (71)$$

The elementary magnetic excitations of the nanoparticle (particle-hole and collective) occur at real frequencies  $\omega$  at which  $\chi_{\alpha\beta}(\omega)$  has poles. Here  $\chi_{\alpha\beta}(\omega)$  is obtained by analytically continuing Eq. (71) to real frequencies:  $i\omega_n \rightarrow \omega + i\eta$ . Let  $D(\omega)$  denote the complex function,

$$D(\omega) = \det[K(\omega)]. \quad (72)$$

The condition for the existence of a pole in  $\chi_{\alpha\beta}(\omega)$  can be expressed by the equation

$$D(\omega) = 0 \quad (73)$$

In order to make progress, we will assume that all the components of  $K$  involving the longitudinal variable  $z$  are small and can be disregarded, except for  $K_{zz}(\omega)$ . The expression for the elementary excitation energy then simplifies to

$$D(\omega) \approx K_{zz} \left[ K_{xx}(\omega) K_{yy}(\omega) - K_{xy}(\omega) K_{yx}(\omega) \right] = 0 \quad (74)$$

where we have used Eqs. (53, 55).

Let us consider first the limit of small nanoparticles, where the single-particle mean-level spacing  $\delta$  is much larger than the ferromagnetic resonance, which is of order the anisotropy energy per atom,  $K$ . In Cobalt  $K \approx 0.1$  meV, and if use bulk single-particle density of states[17] we find that this limit is reached in nanoparticles containing  $N_a \ll 10^4$  atoms. In this case we expect a pure ferromagnetic resonance mode with a large spectral weight that appears as a separate quantum state below the lowest particle-hole excitation energy. (We discuss the situation where particle-hole and collective excitations are not cleanly separated at greater length below.)

Using the expansions of Eqs. (60–62), we obtain

$$\frac{\mathcal{N}_a}{U} \left[ a^2 - b^2 - c^2 - (i\mathcal{C}(\Delta_{\text{MF}}))^2 \omega^2 \right] = 0, \quad (75)$$

which yields a low-energy pole at the real frequency

$$E_{\text{res}} = \frac{\sqrt{a^2 - b^2 - c^2}}{|i\mathcal{C}(\Delta_{\text{MF}})|}. \quad (76)$$

Around the pole we have,

$$[D(\omega)]^{-1} \approx \frac{\mathcal{Z}_{\text{res}}}{E_{\text{res}} - \omega}, \quad (77)$$

where the “residue”  $\mathcal{Z}_{\text{res}}$  is

$$\mathcal{Z}_{\text{res}}^{-1} = 2 \frac{\mathcal{N}_a}{U} \sqrt{a^2 - b^2 - c^2} |i\mathcal{C}(\Delta_{\text{MF}})|. \quad (78)$$

Thus the collective excitations have a gap at  $E_{\text{res}}$ . The gap is proportional to the *quotient* of  $\sqrt{a^2 - b^2 - c^2}$ , which is essentially the total anisotropy energy, and the Berry curvature  $\mathcal{C}(\Delta_{\text{MF}})$ . For particles that are not too small, both quantities are proportional to the particle volume, thus  $E_{\text{res}}$  is approximately independent of particle volume and approximately equal to the anisotropy energy/atom,  $K$ . The spectral weight of the collective mode  $\mathcal{Z}_{\text{res}}$  is inversely proportional to the *product* of the same two quantities. The spectral weight divided by the resonance frequency is proportional to the static response of the exchange-field, a quantity which can be understood simply by minimizing the total micromagnetic energy.

The considerations described above apply when the collective excitation energy is smaller than the lowest energy particle-hole excitation. Even in this limit where particle-hole and collective excitations are well separated, the exchange-field propagator does have some spectral weight in particle hole excitations as well. The Kernel (Eq. 49) must have zeroes between the poles that occur at each mean-field particle-hole excitation energy. Therefore we expect  $D(\omega) = 0$  at  $\omega = \tilde{\omega}_{ji} \approx \omega_{ji} = \xi_I - \xi_J$  and the susceptibility to have additional poles at  $\tilde{\omega}_{ji}$ . Let us expand  $D(\omega)$  around one of these poles

$$[D(\omega)]^{-1} \approx \frac{[D'(\tilde{\omega}_{ji})]^{-1}}{\omega - \tilde{\omega}_{ji}}. \quad (79)$$

Thus, in general the residue of each pole is proportional to

$$\mathcal{Z}_{ji} = [D'(\tilde{\omega}_{ji})]^{-1}. \quad (80)$$

#### D. Coupling between Collective and Particle-hole excitations

If we increase the size of the nanoparticle to a few thousands atoms, the lowest particle-hole excitation energy  $\omega_{ji} \approx \delta$  will start to approach  $E_{\text{res}}$  from above.

In this situation the pole at  $E_{\text{res}}$  will start to lose its collective character. As  $\delta$  becomes much smaller than  $E_{\text{res}}$ , the ferromagnetic resonance mode will no longer be a single excitation, and instead appear as enhanced spectral weight in response functions that is spread over several particle-hole excitations. If we further increase the nanoparticle size such that  $\delta \ll E_{\text{res}}$ , we start to approach the thermodynamic limit, where the collective ferromagnetic resonance will be spread over a large number of particle-hole excitations. If  $E_{\text{res}}$  is the frequency at which Eq. 74 holds, by expanding  $D(\omega)$  near  $E_{\text{res}}$  the ferromagnetic collective mode has a width given by

$$\Gamma = 2 \frac{\text{Im} D(E_{\text{res}})}{\text{Re} D'(E_{\text{res}})}. \quad (81)$$

The susceptibility then has a resonant denominator and ferromagnetic mode has the shape of an asymmetric Lorentzian[26].

It is possible to relate the typical value of matrix elements between single-particle states that appear in the kernel for a *large* nanoparticle and the Gilbert damping parameter usually used to characterize the width of a ferromagnetic resonance line. The Gilbert damping parameter  $\alpha$  is the ratio between the line-width and the resonance frequency. It is normally introduced as a phenomenological damping parameter in Landau-Lifshitz equations of motion for the magnetization direction; these equations are implied by the low-frequency dynamics discussed above. Taking the continuum limit for the particle-hole excitation spectrum and assuming that we have approximate rotational symmetry about the exchange-field-orientation axis, it follows from the preceding analysis that [32]

$$\alpha = \frac{\text{Im}[K_{xx}(\omega = E_{\text{res}})]}{\text{Im}[K_{xy}(\omega = E_{\text{res}})]} \sim \frac{\pi}{2\delta^2 |\mathcal{C}(\Delta_{\text{MF}})|} \overline{|(J|s_x|I)|^2} \quad (82)$$

where the overbar denotes an average over typical particle-hole matrix elements for states near the Fermi energy. Note that  $\alpha$  approaches a constant and the typical matrix element scales like  $\mathcal{N}_A^{-1}$  in the limit of large nanoparticles.

We can estimate the number of individual particle-hole excitations that contribute to the ferromagnetic resonance in a large nanoparticle. The density-of-states for particle-hole excitations grows linearly with energy and at the resonance energy is  $\sim E_{\text{res}}/\delta^2$ . The number of particle-hole excitations in the resonance is the width of the resonance  $\alpha E_{\text{res}}$  times this density of states,  $\sim \alpha E_{\text{res}}^2/\delta^2$ . This expression implies a condition for the crossover to pure-state ferromagnetic resonance when  $\delta = \sqrt{\alpha} E_{\text{res}}$ . The crossover is therefore expected to occur at larger particle sizes when the ferromagnetic resonance is sharp. Even when the particle is small enough that the resonance is not normally coupled with particle-hole excitations, avoided crossings between these two types of excitations will frequently occur as the external magnetic field or other parameters are varied. We

can describe such an avoided crossing by assuming that the low-frequency limit can be taken for all but one of the particle-hole excitation contributions to the kernel. To briefly explain what happens in this limit, for which the kernel can be written as the sum of a part  $K_{xx}^{\text{smooth}}$  with a smooth frequency dependence and a part  $K_{xx}^{\text{res}}$  with a resonant frequency dependence, we assume that the particular particle-hole excitation contributes only to  $K_{xx}^{\text{res}}$ , making a contribution

$$K_{xx}^{\text{res}}(\omega) = \frac{2\omega_{ij}}{\omega^2 - \omega_{ij}^2} |\langle J|s_x|I \rangle|^2. \quad (83)$$

It follows that the poles of the exchange-field propagator occur at energies

$$\omega_{\pm} = \frac{E_{\text{res}} + \omega_{ij}}{2} \pm [[(E_{\text{res}} - \omega_{ij})/2]^2 + V^2]^{1/2} \quad (84)$$

where  $V$  is an avoided crossing gap. Using Eq.( 82) we find that  $V \sim \alpha E_{\text{res}}$ . The size of the avoided crossing gap that occurs in a small nanoparticle when a particle-hole excitation energy is tuned through a collective excitation energy by an external field or another parameter is specified by the ferromagnetic resonance width in the limit of a large particle.

It is important to note that the experiments in Ref. 2, 3 are carried out for nanoparticles containing  $\mathcal{N}_a \approx 1500$  atoms. Thus these experiments are probing the most interesting and *difficult* intermediate regime of particle size, where the lowest particle-hole excitation energy  $\omega_{ji} \approx \delta \rightarrow \sqrt{\alpha} E_{\text{res}}$ .

## V. NUMERICAL RESULTS AND DISCUSSION

In this session we will present numerical calculations performed on our two ferromagnetic nanoparticle models which illustrate and support all the main points of the theory of elementary spin excitations developed above. Since we can deal with nanoparticles containing up to 260 atoms, we expect, on the basis of our theoretical considerations, that the exchange-field correlation function will normally display one main peak at energies below the lowest particle-hole excitation. In addition to verifying this expectation, we will see that the ferromagnetic resonance mode is characterized by a very interesting behavior when manipulated with an external magnetic field to bring it through coincidence with a particle-hole excitation.

As mentioned already in Sec. IV, in discussing the different components of the kernel and the susceptibility we will take the  $z$ -direction along the direction of the magnetization,  $\hat{\Omega}$ . We will also choose the  $y$ -direction to lie in the equatorial  $XY$ -plane of the nanoparticle. Then the  $x$ -direction will be fixed by the condition of being orthogonal to both  $z$  and  $y$ . Therefore the  $x$  and  $y$  components of the kernel describe *transverse* spin fluctuations with respect to the direction of the magnetization, but these

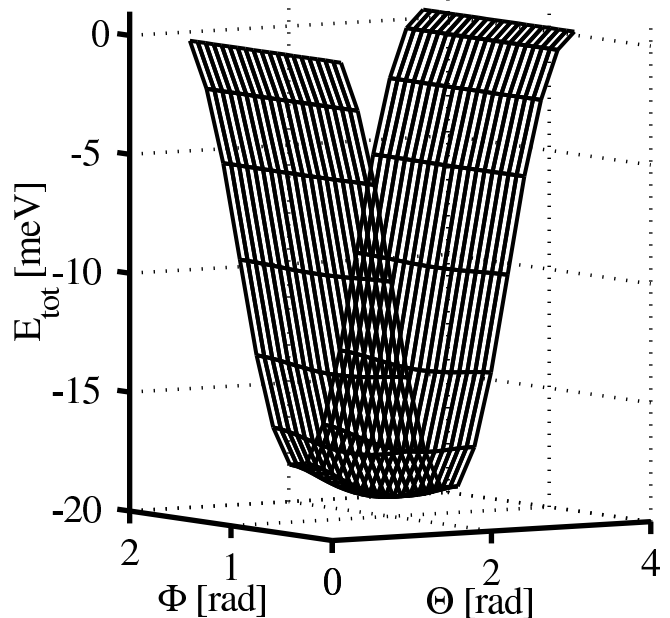


FIG. 2: Anisotropy landscape  $E_{\text{tot}}(\vec{\Delta})$  as a function of  $\Theta$  and  $\Phi$  for a 143-atom hemispherical nanoparticle.  $E_{\text{tot}}$  is periodic in  $\Phi$ , with period  $\pi/2$ .

directions in general will not be symmetry directions with respect to the crystal structure or the nanoparticle geometry. The direction of  $\hat{\Omega}$  is determined by minimizing the classical micromagnetic energy functional  $E_{\text{tot}}(\vec{\Delta})$ , or equivalently by solving the mean-field equations self-consistently. The variation of  $E_{\text{tot}}(\vec{\Delta})$  as a function of  $\Theta$  and  $\Phi$  has been studied in detail in Ref. 7. The main conclusions are summarized in Fig. 2, where we plot  $E_{\text{tot}}(\vec{\Delta})$  in the  $(\Theta, \Phi)$ -plane at  $\vec{H}_{\text{ext}} = 0$  for a hemispherical nanoparticle consisting of  $\mathcal{N}_A = 143$  Co atoms, arranged in a f.c.c. lattice. In this case the magnetization direction  $\hat{\Omega}$  lies in the  $XY$ -plane ( $\Theta = \pi/2$ ), along one of the four directions corresponding to the four degenerate shallow minima of  $E_{\text{tot}}(\vec{\Delta})$ . By applying an external field some of these minima will become classically metastable and we can have different hysteretic behaviors with zero, one or two reversals of the magnetic moment, depending on the direction of the field.

### A. Real part of $K_{xx}(\omega)$

We first consider the spectral representation of the kernel defined in Eq. (49). In Fig. 3(a) we plot  $\text{Re}K_{xx}(i\omega_n)$  vs.  $\text{Re}(i\omega_n)$  – after analytical continuation  $i\omega_n \rightarrow \omega + i\eta$  – for a 26-atom nanoparticle for the case of the LRE model. Consistent with Eqs. (57, 59), for zero SO we find that the Kernel has just one pole at particle-hole excitation energy equal  $\Delta_{\text{MF}}$ , and a gapless zero. With SO interaction included, many more matrix elements  $\langle J|s^+|I \rangle$  will be non-zero, and consequently many more poles corre-

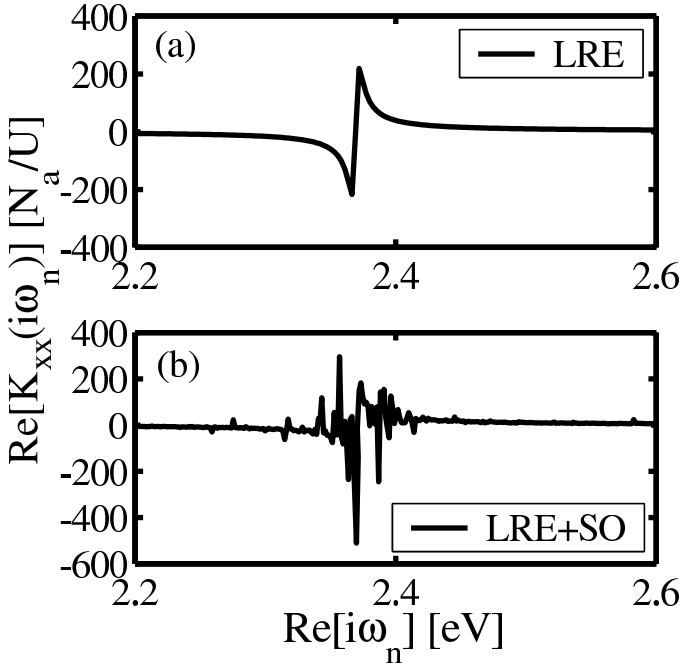


FIG. 3: Real part of the transverse diagonal component of the kernel for a hemispherical 26-atom nanoparticle, Long-Range Exchange model. (a) Without spin-orbit (SO) interaction. (b) With SO interaction.

sponding to these particle-hole excitations will appear in the kernel. This is shown in Fig. 3(b), where we can see that the poles with largest residues still correspond to particle-hole excitations near  $\Delta_{MF}$ . Although not visible in Fig. 3(b) because of its very small residue, the first pole in the kernel occurs at an energy of order of the single-particle mean level spacing  $\delta$ , which for this particle size is approximately 20 meV. This is shown in Fig. 4, where we zoom on a small energy window at very low energies.

Similar results for the LDE model are shown in Fig. (5). We can see [Fig. 5(a)] that the kernel has already several poles even in absence of SO coupling, since not all the energies of majority- and minority-spin states are shifted by the same rigid spin-splitting field, as they were in the case of the LRE model. Most of the poles are still concentrated near  $\Delta_{MF}$ , however. The special properties of the LRE model which result in rigidly split mean-field bands do not, therefore, introduce and special artificial features in the low-energy excitation spectrum. From Fig. 5(b) it would seem that SO interaction do not introduce major effects, merely broadening the pre-existing pole structure. In fact SO interaction changes the analytical structure of the kernel at low energies, as it did for the LRE model. Indeed, Fig. 6 shows that when SO is included the first pole of  $K_{xx}$  occurs again at an energy of the order of the single-particle mean level spacing. We find that most of these low energy particle-hole excitations involve pairs of states that have *mostly* the same *minority* spin character, as expected because

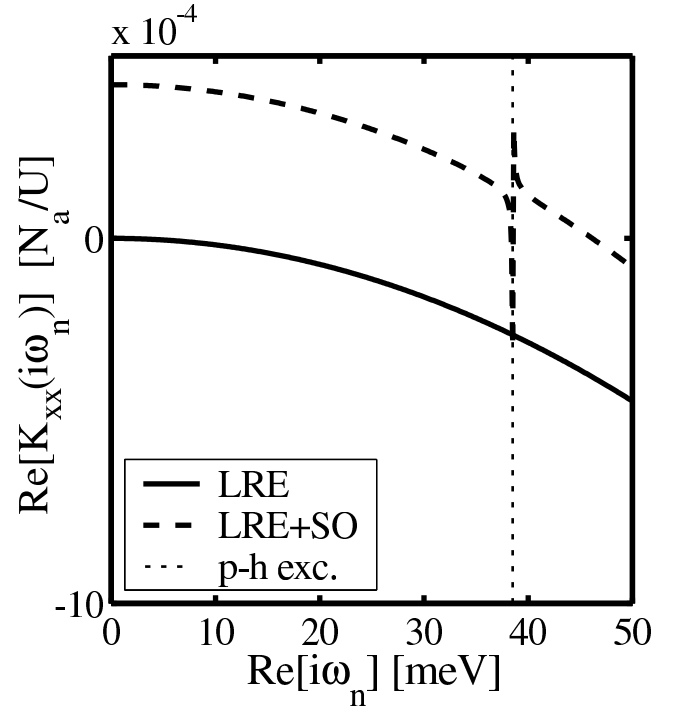


FIG. 4: Low-energy behavior of the Kernel for the same system as in Fig. 3. Solid line: without SO interaction; dashed line: with SO interaction. The vertical dotted line marks the position of the first particle-hole excitation, where  $\text{Re}K_{xx}$  has a pole.

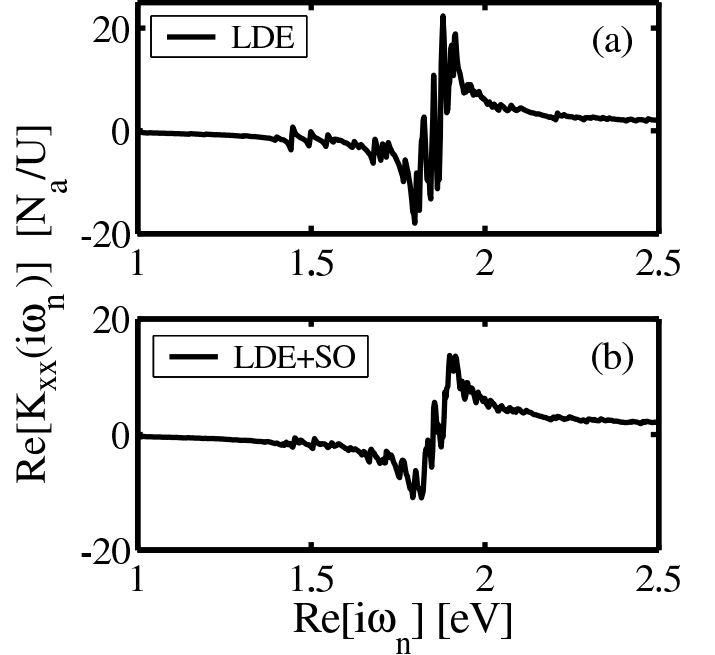


FIG. 5: Real part of the transverse diagonal component of the kernel for a hemispherical 26-atom nanoparticle, Local D-orbital Exchange model. (a) Without SO interaction. (b) With SO interaction.

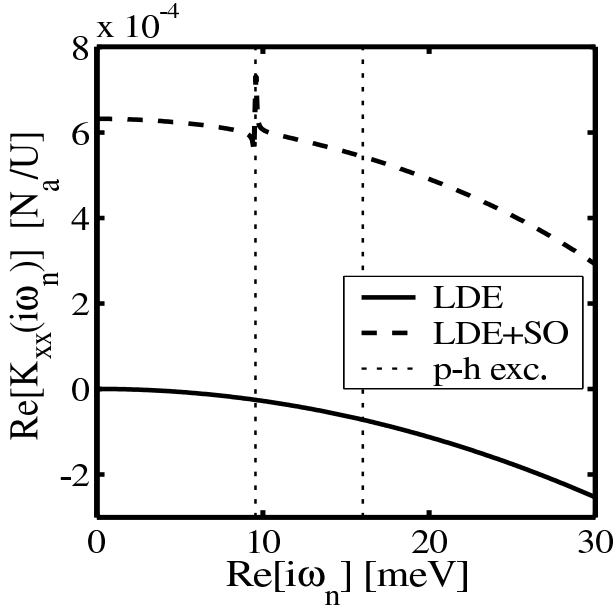


FIG. 6: Low-energy behavior of the Kernel for the same system as in Fig. 5. Solid line: without SO interaction; dashed line: with SO interaction. The vertical dotted lines mark the position of particle-hole excitations.

essentially all states around Fermi level are minority-spin states. Obviously matrix elements  $\langle J, \downarrow | s^+ | I, \downarrow \rangle$  are identically zero and therefore there are no poles at these low energies when SO coupling is not present. It is only when SO coupling is present that these states obtain a small admixture of majority-spin character which produces non-zero matrix elements. It is important to note that even when the rare presence of majority spin states near the Fermi level is recognized, their matrix elements with minority spin states close in energy are always very small because their orbital wavefunctions are almost orthogonal. Fig. 7 shows the low-frequency behavior of the kernel for our two models for the case of a 143-atom nanoparticle. We see essentially the same trend as for the case of smaller nanoparticles: when SO is included the first pole of the Kernel occurs at an energy of the order of the single-particle mean-level spacing, which for this nanoparticle size is of the order of a few meV's. Note that also at this particle size the residue of this low-energy pole is three orders of magnitude smaller than the residues of the poles occurring near  $\Delta_{\text{MF}}$ .

The existence of spin-flip particle-hole excitations at energies of order  $\delta$  has important implications: we will show below that these particle-hole pairs can couple to the low-energy spin collective mode when, by increasing the nanoparticle size and/or by applying an external field, their energy start to approach  $E_{\text{res}}$ .

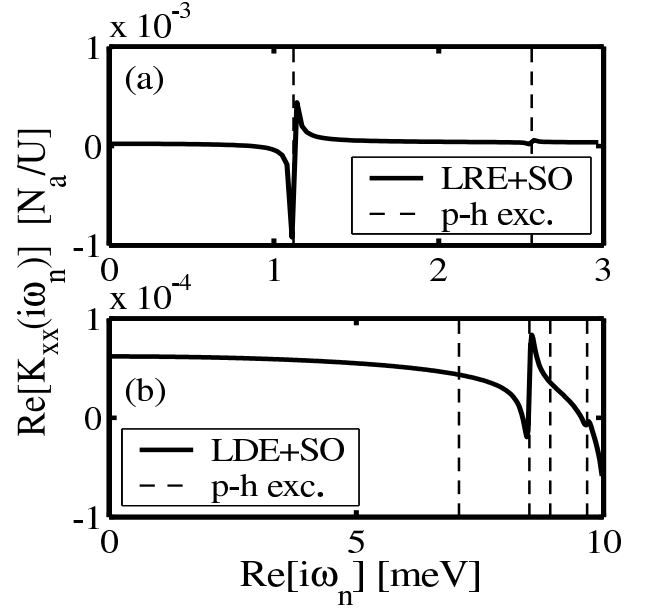


FIG. 7: Real part of the transverse diagonal component of the kernel at low-energies, for a hemispherical 143-atom nanoparticle. (a) Long-Range Exchange model. (b) Local D-orbital Exchange model. Vertical dashed lines mark the position of particle-hole excitations, where  $\text{Re}K_{xx}$  has poles.

### B. Spectral function: $\text{Im}\chi_{xx}(\omega)$ vs. $\omega$

We now discuss the spin-fluctuation spectral function, that is the imaginary part of the spin-susceptibility defined in Eq. (71). In Fig. 8 we plot  $\text{Im}\chi_{xx}(\omega)$  as a function of  $\omega$  for a 143-atom hemispherical nanoparticle for several values of the external magnetic field. As expected from our discussion in Sec. IV, for this nanoparticle size we find that in general the spectral function has only one pole that has substantial weight. At low external fields this pole occurs at a frequency that satisfies Eq. (74), well below the lowest particle-hole excitation. It can therefore be identified as a spin-collective mode. In this regime the collective mode is an exact elementary excitation, at least within the Gaussian approximation that we consider. The finite width in Fig. 8 is due to a finite  $\eta$  in  $i\omega_n \rightarrow \omega + i\eta$ .

Apart from the ferromagnetic resonance pole, the susceptibility has other poles at higher energies, as seen in Fig. 9, where we plot  $D(\omega)$  given in Eq. 74. These poles are all very close to MF particle-hole excitation energies and have virtually zero spectral weight for this particle size, when the external field is zero. We can therefore identify them as the spin-flip particle-hole excitations discussed in Sec. IV C.

As shown in Fig. 8, we can use an external magnetic field to manipulate both energy and spectral weight of the collective mode. From zero field to the reversal field, the collective mode energy and its spectral weight decrease. Beyond the coercive field they both start to increase monotonically. As shown in Fig. 8(b), if we keep

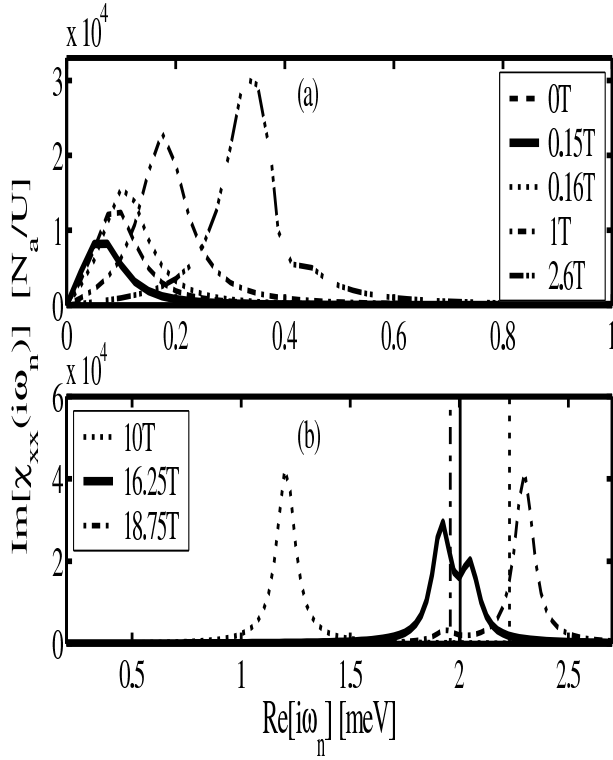


FIG. 8: Imaginary part of the transverse diagonal spin susceptibility ( $x$  component) at different external magnetic fields, for a hemispherical 143-atom nanoparticle in the LDE model.  $\vec{H}_{\text{ext}}$  is in the  $ZX$ -plane at an angle  $\pi/4$  with the  $Z$ -axis.  $H_{\text{ext}} = 0.15$  T is a reversal point. This low-energy peak in the susceptibility corresponds to a spin-collective mode due to coherent magnetization fluctuations. Vertical lines in (b) mark the position of the first particle-hole excitation energy, which shifts down with increasing field. When the collective mode energy approaches the particle-hole excitation energy, the collective mode peak splits and part of its spectral weight is taken away from the pole.

increasing the field, the collective mode energy starts to approach the first particle-hole excitation energy, whose energy decreases with increasing field. When the two energies are proximate to each other, the collective-mode peak splits into two close resonances: part of spectral weight of the magnetization fluctuation is transferred to the nearby particle-hole excitation, as also illustrated in Fig.10 where we plot the derivative of  $D(\omega)$  at  $E_{\text{res}}$  as a function of the external field. The peak in  $D'$  corresponds to a sudden decrease of  $Z_{\text{res}}$  given in Eq. 80: the collective mode can decay into a particle-hole excitation. More precisely, we can say that the two types of excitations are coupled, and therefore it is no longer meaningful to speak about spin-collective modes as distinct from spin-flip particle-hole excitations. In our model the coupling mechanism is provided by the spin-orbit interaction. Indeed, we have checked that without spin-orbit interaction, nothing happens to the collective peak when its energy crosses a particle-hole excitation.

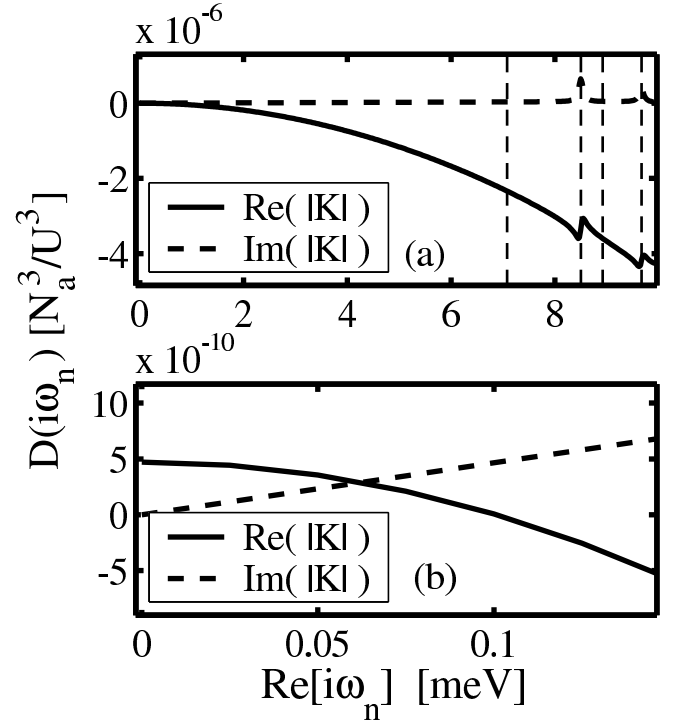


FIG. 9: Determinant of the kernel defined in Eq. 74, for the system of Fig. 8 at zero external field. The first zero of  $\text{Re} D(\omega)$  at  $0.06$  meV corresponds to the ferromagnetic resonance seen in Fig. 8.  $\text{Re} D(\omega)$  has other zero's very close to its poles that are located at particle-hole energies (marked by vertical dashed lines). The zero's correspond to spin-flip particle-hole excitations, but their spectral weight in Fig. 8 is virtually zero unless they approach the ferromagnetic resonance mode.

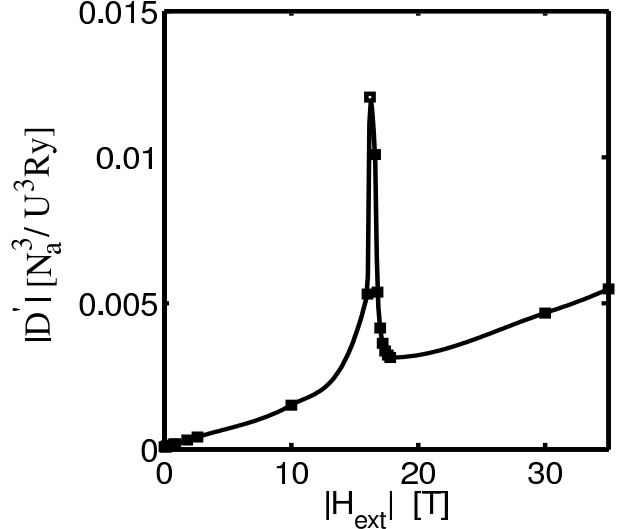


FIG. 10: Derivative of the determinant of the kernel given in Eq. 74, calculated at  $E_{\text{res}}$ , as a function of the external field for the system of Fig.8.  $D'(E_{\text{res}})$  is inversely proportional to the residue of the collective mode. The peak in  $D'(E_{\text{res}})$  occurs where the collective mode energy and the first particle-hole excitation energy cross.

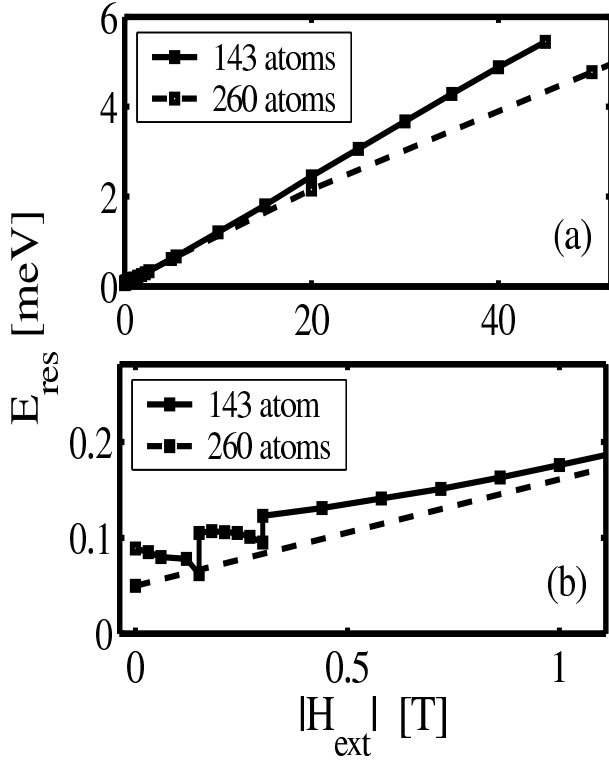


FIG. 11: Variation of the collective-mode energy (low-energy peak in the susceptibility) as a function of the external field for 143-atom and 260-atom nanoparticles.  $\vec{H}_{\text{ext}}$  is in the  $ZX$ -plane at an angle  $\pi/4$  with the  $Z$ -axis. In (b) the detailed low-field behavior is shown. The discontinuities for the 143-atom nanoparticle correspond to magnetization reversal points. (There are no reversal points in the 260-atom system for this external field direction.)

The coupling between collective modes and particle-hole excitations described above mimics what would happen if, instead of manipulating the excitation energies with an external magnetic field, we could progressively increase the size of the nanoparticle up to a few thousand atoms. In this case  $E_{\text{res}}$  would stay approximately constant but  $\delta$  would decrease. When these two energy scales cross the lowest particle-hole excitations will start to interact with the collective mode. It is therefore expected that in a nanoparticle with a few thousand atoms where  $E_{\text{res}} \approx \delta$ , spin collective modes and particle-hole pairs are strongly coupled.

Fig. 11 shows the external field dependence of the energy of the collective mode peak for a 143-atom and a 260-atom nanoparticle respectively. The jumps in the energy for the 143-atom nanoparticle correspond to reversal of the magnetic moment. Interestingly, we have found that the peak energy follows accurately Eq. 76 for all values of the external field, even when its value is larger than the lowest particle-hole energy[33]. The energy gap  $E_{\text{res}}$ , obtained extrapolating the curve at zero field, is approximately volume independent as expected from our general theory. We would like to point out that

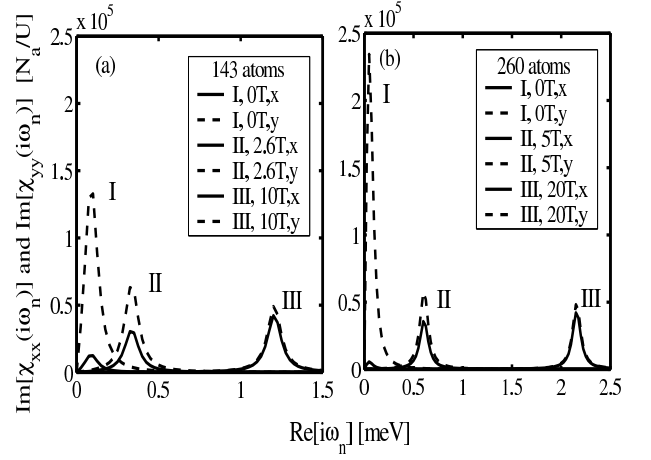


FIG. 12: Imaginary part of the transverse diagonal spin susceptibility,  $x$  and  $y$  components. The external magnetic field is in the  $ZX$ -plane at an angle  $\pi/4$  with the  $Z$ -axis. At high external fields the two transverse components of the spin susceptibility become equal. (a) Hemispherical 143-atom nanoparticle. (b) Hemispherical 260-atom nanoparticle.

at low fields ( $H_{\text{eff}} \leq 1\text{T}$ )  $E_{\text{res}} \sim 0.1\text{ meV}$ , which is of the order of the anisotropy constant/atom  $K$  in Cobalt[8], and is also of the order of the tunneling resonance spacing observed in Refs.2, 3.

### C. Anisotropic Fluctuations

The dynamical susceptibility displays spatial anisotropy in its transverse diagonal components due to the strong anisotropy of the micromagnetic energy functional. We illustrate this point in Fig. 12 by plotting  $\text{Im}\chi_{xx}(\omega)$  together with  $\text{Im}\chi_{yy}(\omega)$ . We can see that also  $\text{Im}\chi_{yy}(\omega)$  has only one dominating collective-mode peak at the same energy of the collective mode in  $\text{Im}\chi_{xx}(\omega)$ . This is obvious since in both cases the collective mode energy is given by Eq. (74). However the *weight* of the pole in the two spectral functions is different and its variation as a function of the external field opposite. At large fields the difference between  $x$  and  $y$  components disappears and the transverse susceptibility becomes isotropic. We find the same trend for hemispherical nanoparticles containing 143 or 260 atoms.

We can get an intuitive understanding of this behavior by looking again at the classical micromagnetic energy functional  $E_{\text{tot}}(\hat{\Omega})$  as a function of  $\Theta$  and  $\Phi$ , shown in Fig. refanisotropy. There are four equivalent minima in the  $XY$  plane at  $\pm\hat{X} \pm\hat{Y}$ , that is  $\Theta = \pi/2$ ,  $\Phi = \pi/4 + n\pi/2$ ,  $n = 1, 2, 3$ . Note however that the energy barrier separating the four minima at  $\Theta = \pi/2$  is very low. We can interpret the collective mode as the zero point motion of a two-dimensional anisotropic harmonic oscillator, whose potential is obtained by expanding  $E_{\text{tot}}(\Theta, \Phi)$  to second-order in  $\Theta$  and  $\Phi$  around



one of the minima. Looking at the  $x$ -component of the spectral function corresponds to exciting the collective oscillation mainly in the hard direction. We can pursue further this analogy and clarify the effect of the external magnetic field. A magnetic field in the  $ZX$  plane starts to decrease the low barriers separating the four minima. Thus the collective mode energy decreases. This continues up to reversal. Note that at reversal the collective mode energy does not go to zero because the potential landscape has only a saddle point there: the potential still increases in the direction of the two poles of the unit sphere ( $\Theta = 0, \pi/2$ ). After the last reversal has taken place, namely once the magnetization has flipped to a stable minimum, a further increase of the magnetic field makes the spring constant of the harmonic oscillator stiffer. Hence the collective mode energy starts to increase. This behavior is summarized in Fig.11. At strong magnetic fields the energy functional is dominated by the Zeeman term and any anisotropy in the transverse fluctuations disappears.

Spherical particles have a more symmetric anisotropy energy landscape, without the strong XY easy plane anisotropy characteristic of hemispherical particles. A reversal point in this case will correspond to the disappearance of the energy barrier in  $E_{\text{tot}}(\hat{\Omega})$  in all directions perpendicular to  $\hat{\Delta}_{MF}$ , or at least a less pronounced saddle point. Therefore spherical nanoparticles show a much stronger decrease of collective mode energies at reversal points.

#### D. Berry Curvature

We conclude this session with a discussion of the numerical results for the Berry curvature  $\mathcal{C}(\Delta_{MF})$  defined in Eq. 29. We have seen that  $\mathcal{C}(\Delta_{MF})$  affects the quantization condition of the collective mode energy given in Eq. 76, and is inversely proportional to its residue, Eq 78. Variations of  $\mathcal{C}(\Delta_{MF})$  from the constant value  $iS/\Delta_{MF}^2$  reflect the non-trivial role played by the spin-orbit interaction. In Fig. 13 we plot  $\mathcal{C}(\Delta_{MF})$  as a function of an external magnetic field for a 143-atom nanoparticle. We have computed  $\mathcal{C}(\Delta_{MF})$  in two different ways, according to Eq. 67 and Eqs. 34-35 respectively. The agreement between the two calculation methods is excellent, especially at low fields [see fig. 13(b)]. The fact that the computation method based on Eq. 35 works well is significant because this method relies only on the knowledge of the ground-state for a given magnetization orientation, which in principle can be obtained with fairly good accuracy from density-functional calculations. Thus Eq. 35 provides a very convenient expression for computing  $\mathcal{C}(\Delta_{MF})$  beyond the mean-field approximation used in the present work, and also for more realistic nanoparticle models.

From Fig. 13 we can see that the external field dependence of  $\mathcal{C}(\Delta_{MF})$  is rather smooth and weak, except when the system approaches a reversal point. At a reversal point  $\mathcal{C}(\Delta_{MF})$  suffers a discontinuous jump. On the other

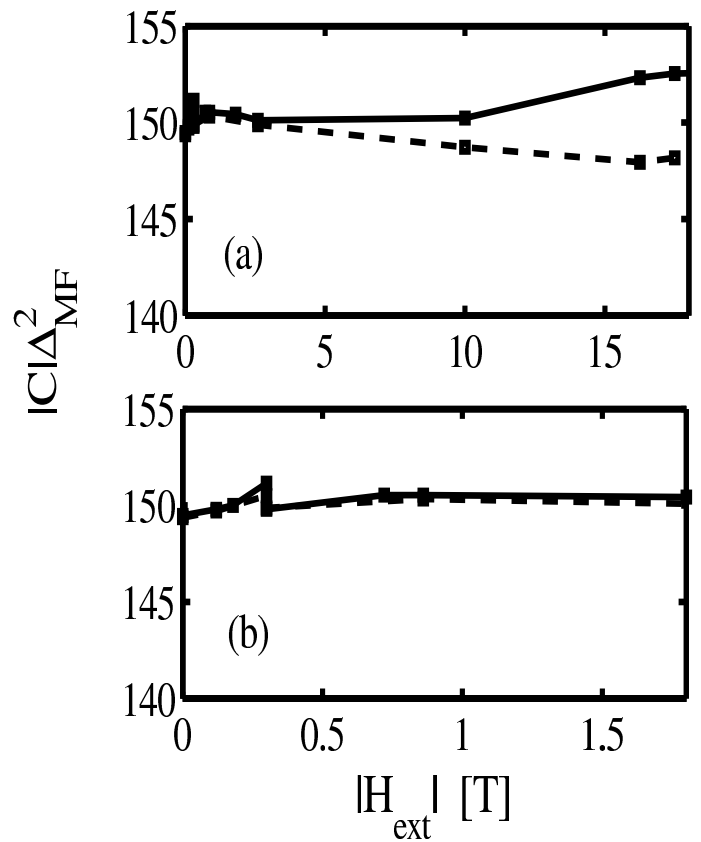


FIG. 13: Berry curvature  $\mathcal{C}(\Delta_{MF})$  for a 143-atom nanoparticle, computed using two different methods: the solid line is obtained from Eq. 67; the dashed line from Eqs. 34-35. (b) Behavior at low fields.

hand,  $\mathcal{C}(\Delta_{MF})$  is completely insensitive to the crossings mentioned above between the ferromagnetic resonance mode and particle-hole excitations, when the latter are of order  $\approx \delta$ . In fact, if we look at the perturbative expression of  $\mathcal{C}(\Delta_{MF})$  given in Eq. 67, we can see that there is no reason to expect any large fluctuations of this quantity when the smallest energy denominator in the sum is  $\approx \delta$ . If the collective mode energy approaches a particle-hole excitation,  $\mathcal{C}(\Delta_{MF})$  will still be well-defined and smooth, but it will not tell us anything about how the collective mode spectral weight is depleted in favor of the nearby particle-hole excitation. In other words, the residue of the collective mode is inversely proportional to  $\mathcal{C}(\Delta_{MF})$  only when the low-frequency expansion is valid, in which case it will be a smooth quantity. When the collective mode energy is close to a particle-hole excitation energy of order  $\delta$ , the low-frequency expansion is meaningless. One must look at the derivative of the determinant  $D(\omega)$  calculated at the pole frequency, given in Eq. 80, to find the residue. An important exception occurs when a particle-hole excitation energy approaches zero (i.e. close to mean-field quasiparticle level crossings)[14]. These are events that can occur only for some particular orientations of the magnetization and at

isolated values of the external fields. When the system is close to a mean-field quasiparticle level crossing, the Berry curvature landscape  $\mathcal{C}(\Delta)$  is strongly distorted. In this case the fluctuations of  $\mathcal{C}(\Delta)$  are a direct indication of the coupling between the collective mode and particle-hole excitations, which obliterate the distinction between them.

## VI. CONCLUSIONS

In summary, we have developed a theory of elementary spin excitations in ferromagnetic metal nanoparticles that provides a consistent and unified quantum description of both quasi-particle and collective mode physics. Our formalism, based on a path integral approach, allows us to make a connection between microscopic exchange and spin-orbit interactions and classical micromagnetic theory. We have shown that small nanoparticles have a collective excitation at energies below the lowest particle-hole excitation energy, whose energy gap  $E_{\text{res}}$  is given by the ratio of the anisotropy energy and the total Berry phase of the system. As the single-particle mean-level spacing decreases and becomes much smaller than  $\sqrt{\alpha}E_{\text{res}}$ , the collective excited states evolves into a damped collective mode whose spectral weight is distributed over a large number of particle-hole excitations.

We have illustrated these ideas by performing numerical calculations of nanoparticles containing up to 260 atoms, described by a microscopic tight-binding model. We have found that for this particle size there is typically an isolated collective excited state below the lowest particle-hole excitation which nearly exhausts the spectral weight of the dynamical susceptibility. The energy gap  $E_{\text{res}}$  is of the order of 0.1meV, and is approximately independent of the particle size. Occasional crossings between primarily single-particle and collective excitations occur as a function of applied magnetic. Near the crossing point, the collective mode peak splits, as a result of resonant coupling between the two types of excitations that is non-zero because of spin-orbit interactions. These crossings become more common as the particles become larger and cannot be avoided for system for nanoparticles with more than typically 10,000 atoms.

Although a detailed comparison with the tunneling transport experiments of Ref. 2, 3 is beyond the scope of the present paper, our analysis sheds light on some essential features which are quite relevant to the understanding of the experimental results. What emerges from our theory is a picture of elementary excitations that is far more complex than that derived from earlier phenomenological models, where the effect of spin-orbit interaction is accounted for only indirectly by means of an uniaxial anisotropy term in a giant spin Hamiltonian that represents the coherent magnetization dynamics. In particular, our results suggest that for the particle size considered in the experiments quasi-particle and spin col-

lective modes are most likely strongly entangled by spin-orbit interactions. It is not unconceivable that such an intertwined set of excitations could provide a rich low-energy tunneling spectrum, even in conditions of equilibrium tunneling.

The energy gap of the ferromagnetic resonance mode can be viewed as the characteristic mean-energy-level spacing between coupled collective-quasiparticle excitations described by an effective Hamiltonian. Interestingly enough, the value of  $E_{\text{res}}$  deduced from our model calculations is of the order of the observed tunneling resonance level spacing. This value, which is also of the order of  $K_{\text{bulk}}$ , is five times larger than the anisotropy constant estimated from the measured switching field using  $K_{\text{sw}} = \mu_B H_{\text{sw}}$ . The smallness of  $K_{\text{sw}}$  is one of the properties that led the authors of Ref.6 to conclude that equilibrium spin excitations involving only the lowest spin-multiplet cannot be resolved in the present experiments and therefore cannot explain the observed large density of resonances. While the discrepancy between  $K_{\text{sw}}$  and  $K_{\text{bulk}}$  is still a puzzle[27] (see however [34]), our results suggest that these low-lying excitations are in fact being detected. These considerations do not necessarily imply that the main features of the tunneling experiments can be understood by equilibrium transitions alone. Measurements on gated devices[3] convincingly support the hypothesis that non equilibrium transitions play a crucial role. The point that we want to make here is that low-lying *equilibrium spin excitations* are probably equally important for the interpretation of the experimental results.

It would be highly desirable to perform new tunneling experiments in more controlled situations and especially with smaller nanoparticles, so that the spin excitations associated with the electronic degrees of freedom and with the magnetization collective coordinate could be more easily disentangled. The physical condition required to reach this regime is that the single-particle mean level spacing be larger than the total anisotropy energy[14]. For Cobalt this would imply dealing with nanoparticles containing of the order of 100 atoms, which is within reach of the present experimental capabilities.

## VII. ACKNOWLEDGEMENTS

We would like to thank Mandar Deshmukh and Dan Ralph for several discussions about their experimental results, Jan von Delft and Piet Brouwer for stimulating and informative interactions. This work was supported in part by the Swedish Research Council under Grant No:621-2001-2357, by the faculty of natural science of Kalmar University, and in part by the National Science Foundation under Grants DMR 0115947 and DMR 0210383. Support from the Office of Naval Research under Grant N00014-02-1-0813 is also gratefully acknowledged.

- 
- [1] J. von Delft and D. C. Ralph, *Spectroscopy of discrete energy levels in ultrasmall metallic grains* (2001).
- [2] S. Guéron, M. M. Deshmukh, E. B. Myers, and D. C. Ralph, Phys. Rev. Lett. **83**(20), 4148 (1999).
- [3] M. M. Deshmukh, S. Kleff, S. Guéron, E. Bonnet, A. N. Pasupathy, J. von Delft, and D. C. Ralph, Phys. Rev. Lett. **87**(22), 226801 (2001).
- [4] C. M. Canali and A. H. MacDonald, Phys. Rev. Lett. **85**(26), 5623 (2000).
- [5] S. Kelff, J. von Delft, M. M. Deshmukh, and D. C. Ralph, Phys. Rev. B **64**, 220401 (2001).
- [6] S. Kleff and J. von Delft, Phys. Rev. B **65**, 214421 (2002).
- [7] A. Cehovin, C. M. Canali, and A. H. MacDonald, Phys. Rev. B **66**(10), 94430 (2002).
- [8] M. B. Stearns, in *3d, 4d and 5d Elements, Alloys and Compounds*, edited by H. Wijn and Landolt-Brstein (Springer, Berlin, 1986), vol. 19 of pt. a of *New Series, Group III*, p. 34.
- [9] V. Korenman and R. E. Prange, Phys. Rev. B **6**, 2769 (1972).
- [10] V. Korenman, Phys. Rev. B **7**, 3147 (1974).
- [11] J. F. Cooke, J. W. Lynn, and H. L. Davis, Phys. Rev. B **21**(9), 4118 (1980).
- [12] A. H. MacDonald and C. M. Canali, Solid State Comm. **119**, 253 (2001).
- [13] T. L. Gilbert, Phys. Rev. **100**, 1243 (1955).
- [14] C. M. Canali, A. Cehovin, and A. H. MacDonald, *Chern numbers for spin models of transition metal nanomagnets* (2003), cond-mat/030355.
- [15] J. C. Slater and G. F. Koster, Phys. Rev. **94**(6), 1498 (1954).
- [16] L. F. Mattheiss, Phys. Rev. B **2**(10), 3918 (1970).
- [17] D. A. Papaconstantopoulos, *Handbook of the Band Structure of Elemental Solids* (Plenum, New York, 1986).
- [18] D. D. Koelling and A. H. MacDonald, in *Relativistic Effects in Atoms, Molecules and Solids*, edited by G. L. Malli (Plenum Publishing Corporation, New York, 1983), vol. 87 of *NATO Advanced Study Institute, Ser. B*, p. 227.
- [19] K. B. Efetov, *Supersymmetry in disorder and Chaos* (Cambridge University Press, Cambridge, 1997).
- [20] A. Auerbach, *Interacting electrons and quantum magnetism* (Springer-Verlag, New York, 1994).
- [21] E. Fradkin, *Field Theories of Condensed Matter Systems* (Addison-Wesley, Redwood City, 1991).
- [22] Q. Niu and L. Kleinman, Phys. Rev. Lett **80**(10), 2205 (1998).
- [23] Q. Niu, X. Wang, L. Kleinman, W. M. Liu, D. M. C. Nicholson, and G. M. Stocks, Phys. Rev. Lett **83**(1), 207 (1999).
- [24] T. Oda, A. Pasquarello, and R. Car, Phys. Rev. Lett. **80**(16), 3622 (1998).
- [25] A. Cehovin, *Nonhomogenous self-consistent hartee-fock approximation in ferromagnetic metal nanoparticles* (2001), unpublished.
- [26] J. Callaway, A. K. Chatterjee, S. P. Singhal, and A. Zoegler, Phys. Rev. B **28**(7), 3818 (1983).
- [27] M. M. Deshmukh, *Probing magnetism at the nanometer scale using tunneling spectroscopy* (2002), ph. D. thesis, Cornell University 2002. <http://www.ccmr.cornell.edu/mandar/mandar-thesis.ps.gz>.
- [28] S. Ingvarsson, L. Ritchie, X. Y. Liu, G. Xiao, C. S. J, P. L. Trouilloud, and R. H. Koch, Phys. Rev. B **66**, 214416 (2002).
- [29] V. L. Safonov and H. N. Bertram, *Microscopic relaxation mechanisms and linear magnetization dynamics* (2002), con-mat/0207721.
- [30] In this paper we will focus on the damping of the uniform collective mode arising from the decay into particle-hole excitations. There are of course other important sources of damping not considered here, for example magnetoelastic scattering by phonons and magnon-magnon interactions enhanced by surface defects. Some of these relaxation mechanisms have been investigated recently both experimentally[28] and theoretically[29].
- [31] We will use  $X$ ,  $Y$  and  $Z$  to indicate the directions of the f.c.c. crystal axes.
- [32] In the continuum limit the imaginary part of  $K_{xx}$  and  $K_{yy}$  will have terms linear in  $\omega$ , which cause the ferromagnetic resonance mode to have a finite lifetime.
- [33] The only exception is when a particle-hole excitation energy exactly crosses the collective mode peak. As we have explained, in this case the two excitations are coupled and there is a small splitting separating them.
- [34] One possible explanation that we have put forward in Ref. [7] is that under the action of an external field, small groups of atoms can change their orientation relative to other parts of the nanoparticle. The small  $K_{sw}$  extracted from tunneling experiments would then refer to such local reorientation processes.